

# **Investigations on Generation of Copper Nanoparticles by Pulsed Electrolytic Dissolution**

**M.Tech Thesis**

*By*

**Muneer Alam**



**Discipline of Mechanical Engineering  
Indian Institute of Technology Indore**

**July 2016**



# **Investigations on Generation of Copper Nanoparticles by Pulsed Electrolytic Dissolution**

**A Thesis**

*Submitted in partial fulfillment of the  
requirements for the award of the degree*

*of*

**Master of Technology**

*In*

**Mechanical Engineering**

with specialization in

**Production and Industrial Engineering**

*by*

**Muneer Alam**



**Discipline of Mechanical Engineering  
Indian Institute of Technology Indore**

**July 2016**





# Indian Institute of Technology Indore

## Candidate's Declaration

I hereby certify that the work which is being presented in the thesis entitled **“Investigations on Generation of Copper Nano-particles by Pulsed Electrolytic Dissolution Process”** in the partial fulfillment of the requirements for the award of the degree of **Master of Technology in MECHANICAL ENGINEERING** with specialization in **PRODUCTION and INDUSTRIAL ENGINEERING** and submitted in the **Discipline of Mechanical Engineering, Indian Institute of Technology Indore**, is an authentic record of my own work carried out during the time period from May 2015 to June 2016 under the supervision of **Prof. Neelesh Kumar Jain** and **Dr. I A Palani** of Discipline of Mechanical Engineering.

The matter contained in this thesis has not been submitted by me for the award of any degree from any other institute.

**Muneer Alam**

-----  
This is to certify that the above statement made by the candidate is correct to the best of our knowledge.

**Dr. I. A. Palani**

**Prof. Neelesh Kumar Jain**

-----  
**Muneer Alam** has successfully completed his M.Tech Oral Examination, held on .....

Signature of M.Tech Thesis Supervisors

Date:

Signature of Convener, DPGC

Date:

Signature of PSPC Member 1

Date:

Signature of PSPC Member 2

Date:

-----  
Signature of Chairman, Oral Examination Board with date



## Acknowledgements

I take this opportunity to express my deep sense of respect and gratitude toward **Prof. N. K. Jain** and **I.A Palani**, for believing in me to carry out this work under their supervision. Their constant encouragement and constructive support have enabled this work to achieve its present form. Innovative perspective of Prof. Jain towards things and his continuous pursuit for perfection has had a profound effect on me and has transformed me majorly. I feel greatly privileged to be one of his students.

My gratitude is also extended towards my PSPC members **Dr. Santosh Kumar Sahu** and **Dr. Vipul Singh** for their guidance and cooperation. I am grateful to the **Prof. Pradeep Mathur, Director, IIT Indore** and **faculty members** of Discipline of **Mechanical Engineering** for providing the essential facilities and guidance.

I would like to express my recondite thanks to my senior **Mr. Sunil Pathak** for his moral support and the not-so-serious moments shared between us have been highly beneficial during the hardships of this project. I express my deep sense of gratitude to **Sujeet Choubey, Mayur Sawant, Sagar Nikam** for bearing with me and always maintaining a homely atmosphere in the lab. Special thanks are extended to my colleagues, **Akshay Namdeo, Priya Chouhan, Vinayak Yadav, Swagat Dwibedi, Pravin Rai, Rohit Gagrani, Vibhore pandhare, Naresh Kumar Wagri, Mridul Upadhyay, Jitendra Singh and Jitesh Bhojar** for their help, suggestions whenever I needed and for always giving me company, and to all the M.Tech 2016, Production and Industrial Engineering (PIE) batch.

I am also thankful to Lab staff of Mechanical Engineering Labs and Central Workshop, specially **Anand Petare ASW, IIT Indore, Santosh Sharma and Sandeep Gour, Mr. Umakant Sharma, Mr. Pawan Chouhan, Mr. Satish, Mr. Deepak Rathore, Mr Vinay Misra** for their cooperation in fabrication of my experimental setup.

Last, but not least, I would like to dedicate this thesis to **my parents, my brother and sister** for their love, patience, and understanding. Because without their support, I would have never reached where I am today.

**Muneer Alam**



*Dedicated to my Family*



## **Abstract**

This thesis reports a simple, novel, cost effective and eco-friendly electrolytic synthesis of copper nanoparticles using copper sulphate as metal precursor. The synthesis rate is much faster than other methods and this approach is suitable for large scale production. Generated nano-particles were characterized by X-ray diffraction (XRD), scanning electron microscope and Energy-dispersive X-ray spectroscopy (EDX) to analyze size, morphology and chemical composition of the particles.

The experimental work was divided into pilot and main experiment. The pilot experiments were conducted to study the effect of electrolyte concentration, inter electrode gap (IEG) and time on the nano-particles shape and size. Average minimum size of the particles in the pilot experiments were found to be 150 nm at identified optimum value of the parameters; 5 wt.% of electrolytic concentration; 30 minutes of operating time; and 10 mm of IEG. The main experiments were conducted to optimize the size of the particles to avoid agglomeration of the particles. Average minimum size of the particles in the main experiments was found to be 70 nm at identified optimum value of the parameters; 8 V of voltage; 4 ms of pulse-on time and 8 ms of pulse-off time. Shape of the particles was found to be irregular. There was no direct linear relationship between these six parameters. XRD results shows three peaks at  $2\theta$  values of 44, 51 and 74 deg corresponding to (111), (200), and (220) planes of copper. Peaks obtained are sharp which show copper particles are highly crystalline. The particles size was in the range of 70 nm to 800 nm and irregular in shape.



# CONTENTS

Page No.

|   |              |
|---|--------------|
| <b>List of Figures .....</b>  | <b>ix</b>    |
| <b>List of Tables .....</b>   | <b>xi</b>    |
| <b>Nomenclature .....</b>   | <b>xiii</b>  |
| <b>Organization of the Thesis .....</b>                                 | <b>xv</b>    |
| <b>Chapter 1: Introduction .....</b>                                    | <b>1-9</b>   |
| 1.1 Importance of Nano-particles .....                                  | 2            |
| 1.2 Properties of Nano-particles .....                                  | 3            |
| 1.3 Difference in Properties of Nano-particles and Bulk Materials ..... | 4            |
| 1.4 Methods of Generation of Nano-particles .....                       | 4            |
| 1.5 Applications of Copper Nano-particles .....                         | 7            |
| 1.6 Introduction to Electrochemical Dissolution Process .....           | 7            |
| 1.6.1 Process parameters of Pulsed-ECD .....                            | 8            |
| <b>Chapter 2: Review of Past Work and Research Objectives .....</b>     | <b>11-17</b> |
| 2.1 Review of Past Work on Generation of Nano-particles .....           | 12           |
| 2.2 Identified Research Gaps .....                                      | 16           |
| 2.3 Research Objectives of Present Work .....                           | 16           |
| 2.4 Research Methodology .....  | 17           |
| <b>Chapter 3: Development of Experimental Apparatus .....</b>           | <b>19-23</b> |
| 3.1 Development and Working of Experimental Apparatus .....             | 19           |
| 3.1.1 Power Supply Unit .....   | 21           |
| 3.1.2 Electrodes .....  | 22           |
| 3.1.3 Mechanism for Adjusting Inter-electrode Gap .....                 | 22           |
| 3.1.4 Housing of Experimental Apparatus .....                           | 23           |
| 3.2 Selection of Material for Electrodes .....                          | 23           |
| 3.3 Selection of Electrolyte .....                                      | 23           |

|   |              |
|---|--------------|
| <b>Chapter 4: Planning of Experimental Investigations .....</b> | <b>25-27</b> |
| 4.1 Planning of Pilot Experiments .....                         | 25           |
| 4.2 Planning of Main Experiments .....                          | 26           |
| 4.3 Characterization of Nano-particles .....                    | 27           |
| 4.4 Procedure of Experimentation .....                          | 27           |
| <b>Chapter 5: Results and Discussion .....</b>                  | <b>29-54</b> |
| 5.1 Pilot Experiments .....                                     | 29           |
| 5.1.1 Effect of Electrolyte Concentration .....                 | 35           |
| 5.1.2 Effect of Inter-electrode Gap .....                       | 37           |
| 5.1.3 Effect of Time .....                                      | 40           |
| 5.2 Main Experiments .....                                      | 42           |
| 5.2.1 Effect of Voltage .....                                   | 47           |
| 5.2.2 Effect of Pulse-on Time and Pulse-off Time .....          | 50           |
| 5.3 Analysis of Chemical Composition and Morphology .....       | 53           |
| <b>Chapter 6: Conclusions and Scope for Future Work .....</b>   | <b>55-56</b> |
| 6.1 Conclusions.....  | 55           |
| 6.2 Scope for Future Work .....                                 | 56           |
| <b>References .....</b>   | <b>57</b>    |
| <b>Appendix-A: Details of the Instrument Used .....</b>         | <b>61</b>    |

## List of Figures

| <b>Figure Number and its Caption</b>   | <b>Page No.</b> |
|--|-----------------|
| <b>Fig.1.1:</b> Application of nano-particles in different fields .....  | 2               |
| <b>Fig. 1.2:</b> Increase in surface area as cube is cut into 8 pieces .....   | 4               |
| <b>Fig. 1.3:</b> Different methods for generation of nano-particles. ....  | 5               |
| <b>Fig 1.4:</b> Schematic representation of rectangular pulse in PECD process .....  | 9               |
| <b>Fig 2.1:</b> Research methodology used in the present work .....  | 17              |
| <b>Figure 3.1:</b> The developed experimental apparatus: (a) schematic diagram;<br>(b) photograph .....  | 20              |
| <b>Fig. 3.2:</b> Photograph of the pulsed DC power supply .....  | 21              |
| <b>Fig. 3.3:</b> Photograph of the oscilloscope .....  | 22              |
| <b>Fig. 3.4:</b> Photograph of the mechanism to adjust the IEG .....   | 22              |
| <b>Fig. 4.1:</b> Box-Behnken experimental design for three parameters varying at<br>three levels each .....  | 26              |
| <b>Fig 4.2:</b> Procedure to generate nano-particles by ECD.....   | 27              |
| <b>Fig.5.1:</b> Effect of electrolyte concentration on average size of copper nano-<br>particles.....  | 35              |
| <b>Fig. 5.2:</b> SEM images of the copper nano-particles generated in 45 minutes<br>using IEG as 10 mm (a) agglomerated nano-particles using electrolyte<br>concentration as 10%; nano-particles with reduced agglomeration using<br>electrolyte concentration (b) 7.5%; and (c)<br>5%.....          | 36              |
| <b>Fig. 5.3:</b> Photographs of the thin layer of copper coated on the cathode plate<br>in 1 hr by PECD process using 50% electrolyte concentration (front view); (b)<br>side view showing thickness of thin film of copper. ....  | 37              |
| <b>Fig. 5.4:</b> Effect of inter-electrode gap on average size of copper nano-<br>particles.....   | 38              |
| <b>Fig. 5.5:</b> SEM images of the copper nano-particles generated in electrolyte<br>concentration 7.5 wt.% using time as 15minutes (a) agglomerated nano-<br>particles using IEG as 5 mm; nano-particles with reduced agglomeration<br>using electrolyte concentration (b) 10mm; and (c) 15 mm..... | 39              |
| <b>Fig. 5.6:</b> Effect of operating time on average size of copper nano-particles ...   | 40              |
| <b>Fig. 5.7:</b> SEM images of the copper nano-particles generated in electrolyte<br>concentration 10 wt.% using IEG as 10mm (a) agglomerated nano-particles   | 41              |

|  |    |
|--|----|
| using operating time as 45 minutes; nano-particles with reduced size of the particles using operating time (b) 30minutes.....  |    |
| <b>Fig. 5.8:</b> Effect of voltage on average size of copper nano-particles .....  | 49 |
| <b>Fig. 5.9:</b> SEM images of the copper nano-particles generated in pulse-on time 6 ms using pulse-off time as 4 ms (a) agglomerated nano-particles using voltage as 16V; nano-particles with reduced size of the particles using voltage (b) 8V.....        | 50 |
| <b>Fig. 5.10:</b> (a) Effect of pulse-on time on average size of copper nano-particles (b) Effect of pulse-off time on average size of copper nano-particles.....  | 51 |
| <b>Fig. 5.11:</b> SEM images of the copper nano-particles generated in Voltage 8V using pulse-off time as 8 ms (a) agglomerated nano-particles using pulse-on time as 6 ms; nano-particles with reduced size of the particles using pulse-on time (b) 4ms..... | 52 |
| <b>Fig. 5.12:</b> XRD analysis of copper nano-particles.....   | 54 |
| <b>Fig. 5.13:</b> Elemental distribution of the material .....   | 54 |

## List of Tables

| <b>Table Number and its Caption</b>  | <b>Page No.</b> |
|--|-----------------|
| <b>Table 1.1:</b> Definitions of nano-particles and nano-material by various organizations ( <b>Horikoshi and Serpone, 2013</b> ) .....                              | 1               |
| <b>Table 2.1:</b> Summary of material applications, limitations, advantages of different methods of nano-particles generation used in past .....                     | 11              |
| <b>Table 2.2:</b> Summary of past work on generation of nano-particles .....   | 12              |
| <b>Table 4.1:</b> Details of variable and fixed parameters, their selection criteria and responses used in the pilot experiments .....                               | 25              |
| <b>Table 4.2:</b> Details of variable and fixed parameters and responses used in the main experiments .....  | 26              |
| <b>Table 5.1:</b> Average size of the generated copper nano-particles and their SEM images for different input parameters combinations in 15 pilot experiments. .... | 30              |
| <b>Table 5.2:</b> Average size of the generated copper nano-particles and their SEM images for different input parameters combinations in 27 main experiments.....   | 42              |
| <b>Table 6.1:</b> Process parameters and range of the particles obtained from main and pilot experiments .....   | 54              |



## Nomenclature

|                        |   |
|------------------------|---|
| <b>V</b>               | Voltage(V)                              |
| <b>t</b>               | Operating time (minutes)                |
| <b>T<sub>on</sub></b>  | Pulse-on time(minutes)                  |
| <b>T<sub>off</sub></b> | Pulse-off time(minutes)                 |
| <b>C</b>               | Concentration (wt. %)                   |
| <b>ECD</b>             | Electro chemical dissolution            |
| <b>IEG</b>             | Inter Electrode Gap (mm)                |
| <b>SEM</b>             | Scanning electron microscope            |
| <b>XRD</b>             | X-Ray Diffraction                       |
| <b>FTIR</b>            | Fourier transform infrared spectroscopy |
| <b>UV-vis</b>          | Ultraviolet-visible spectroscopy        |



# Organization of the Thesis

This thesis is organized into SIX chapters with following contents:

**Chapter 1** details applications of nanoparticles, different synthesis methods to generate nanoparticles challenge, concept of Electro Chemical Dissolution, its parameters, advantages and limitations.

**Chapter 2** presents review of past work on nanoparticles synthesis using different processes, research gaps identified based on this review and the research objectives defined based on the identified research gaps.

**Chapter 3** presents the fabrication of the experimental setup, different sub-systems and the components used in the development of the experimental apparatus and working of the experimental setup.

**Chapter 4** describes planning and details of experiments carried out for the present work. It presents the planning and designing of pilot and main experiment.

**Chapter 5** presents experimental results and their analysis focusing on the effects of variable parameters on the nanoparticles shape and size with identification of optimum level of the process parameters. It also presents analysis of SEM and XRD results.

**Chapter 6** highlights the conclusions derived from the present work and scope for future work based on the limitations of the present work.

# Chapter 1

## Introduction

Particles can be classified according to their size. Particles having size in the range from 2500 to 10,000 nm are called coarse particles, particles having size in the range from 100 to 2500 nm in size are called fine particles and particles having size in the range of 1 to 100 nm are known as ultra-fine particles or nano-particles. Definition and concept of a nano-particle highly depends on a particular application. Table 1.1 presents definitions of nano-particles and nano-materials by various organizations. More generic definition of nano-particles can be *particles which have structured components with size less than 100 nm at least in one dimension*. A nano-particle is the most fundamental component in the synthesis of a nano-structure and is far smaller than the worldly objects for which Newton's law of motion are applicable but bigger than an atom or simple molecule that are governed by quantum mechanics (**Horikoshi and Serpone 2013**). Metallic nano-particles differ from bulk metals in chemical and physical properties (e.g., lower melting points, higher specific surface areas, mechanical strength and specific optical properties) that might prove attractive in various industrial applications. Nano-particles are currently an area of intense scientific research due to wide variety of potential applications in the field of biomedical, optical, and electronic field.

**Table 1.1:** Definitions of nano-particles and nano-material by various organizations (**Horikoshi and Serpone, 2013**).

| Organizations  | Definition of nano-particle   | Definition of nano-material                                |
|--|---|--|
| International Organization for Standardization (ISO)         | A particle spanning 1–100 nm in diameter  | –  |
| American Society of Testing and Materials (ASTM)             | An ultra-fine particle whose length in 2 or 3 places is in the range of 1–100 nm              | –  |
| National Institute of Occupational Safety and Health (NIOSH) | A particle with diameter in the range of 1 to 100 nm, or a fiber spanning the range 1–100 nm. | –  |
| Scientific Committee on Consumer Products (SCCP)             | At least one side is in the nano-scale range  | Material for which at least one side or internal           |
| British Standards Institution (BSI)                          | All the fields or diameters are in the nano-scale range.                                      | structure is in the nano-scale                             |
| Bundesanstalt für Arbeitsschutz und Arbeitsmedizin (BAuA)    | All the fields or diameters are in the nano-scale range                                       | Material consisting of a nanostructure or a nano-substance |

## 1.1 Importance of Nano-particles

During past decade, nano-particles have generated curiosity in many fields such as physics, chemistry, medical science and engineering science. They exhibit enhanced size-dependent properties as compared to larger particles of the same material. They are invisible so transparent coating /film are attainable. They are very weight-efficient so surface can be modified with minimal material. The role of nano-materials in modern technologies is becoming increasingly significant because of feasibility and ease of adding new functions to the existing commercial products. These materials have created a high interest in recent years by their better mechanical, electrical, optical and magnetic properties (Nekouei *et al.*, 2013). Nano-technology is an advanced technology, which deals with the synthesis of nano-particles, processing of the nano-materials and their applications. It considers a particle as a small object that behaves as a whole unit with respect to its transport and properties. It exploits the advantages of ultra-small size, enabling the use of particles to deliver a range of important benefits. There are many applications of nano-particles and its derived products. Figure 1.1 presents applications of the nano-particles in different fields while, following paragraphs mentions some specific applications.

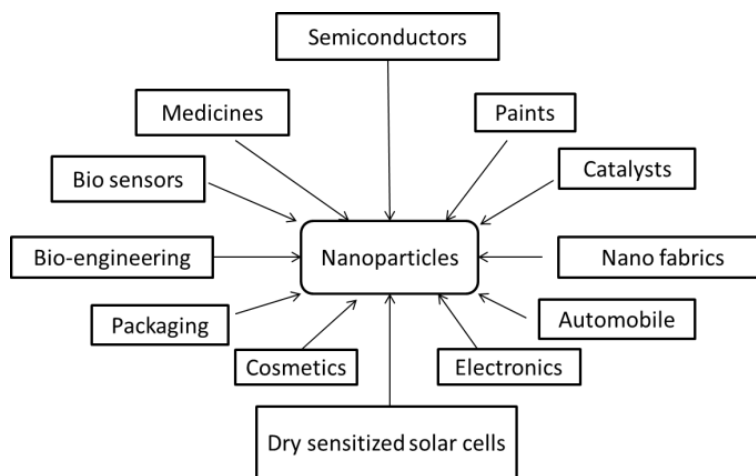


**Fig 1.1:** Application of nano-particles in different fields.

- ❖ **Biomedical & Healthcare:** Nano-scale biosensors and imaging, nano-coatings on surfaces and implants, and nano particulate drug delivery.
- ❖ **Electronics:** Carbon nanotubes, nano-wires, nano-scale memory, printed electronics, NEMS (nanoelectromechanical system)
- ❖ **Textiles:** Coatings, smart materials and sensors, nano-fibres;
- ❖ **Food agriculture:** Nano-sensors, encapsulation, nano-coatings, nano-composites and non-porous membranes.

- ❖ **Energy:** Photovoltaic film coatings, fuel cells and batteries, thermoelectric materials, and aerogels.
- ❖ **Environmental:** Nano-porous membranes, chemical and bio nano-sensors, nano-particles and nano-coatings.
- ❖ **Construction:** Nano-scale sensors and smart materials, nano-composites, nano-coatings and additives to concrete.
- ❖ **Aerospace and defense:** Nano-composites, electronics and sensors, nano-coatings, energy devices & fuel additives and smart materials.
- ❖ **Automotive:** Nano-coatings, composite fillers, additives in catalysts and lubricants, fuel cells and smart materials.

## 1.2 Properties of Nano-particles

Nano-particles are a bridge between bulk materials and atomic or molecular structures. A bulk material should have constant physical properties regardless of its size, but at the nano-scale size-dependent properties are often observed. Thus, the properties of materials change as their size approaches to nano-scale and as the percentage of atoms at the surface of a material becomes significant. For bulk materials larger than one micrometer, the percentage of atoms at the surface is insignificant in relation to the number of atoms in the bulk of the material. Interesting and sometimes unexpected properties of nano-particles are due to large surface area of the material which dominates the contribution made by small bulk material. Nano-particles often possess unexpected optical properties as they are small enough to confine their electrons and produce quantum effects. Absorption of solar radiation is much higher in materials composed of nano-particles than it is in thin films of continuous sheets of material. Suspension of particles are possible because of interaction of particles with solvent is strong enough to overcome density difference otherwise it results in floating of material in liquid. Nano-particles provide super magnetism to magnetic materials. Change in physical properties of a material is not always desirable. Ferromagnetic materials smaller than 10 nm can switch their magnetization direction using room temperature thermal energy, thus making them unsuitable for memory storage. Nano-particles provide a tremendous driving force for diffusion because of high surface to volume ratio at elevated temperature. For small size of particles, sintering can take place at lower temperature over shorter period of time as compared to large size of particles. Semiconducting nano-particles may be labeled as quantum dots are used in biomedical application such as drug carriers if they are small enough that quantization of electronic energy levels occurs.

### 1.3 Difference in Properties of Nano-materials and Bulk Material

Nano-particles are so small that they have different properties than the same substance in normal-sized pieces. For example, pieces of gold are, fairly obviously, gold-colored. But gold nano-particles are deep red or even black when mixed with water. Such different properties are very useful. Nano-scale materials have far larger surface area than similar masses of larger scale materials. As surface area per mass increases, a greater amount of material comes into contact with surrounding material, thus affecting reactivity. At nano-scale particle-particle interaction is dominated by weak Vander Wall forces, stronger polar and electrostatic interaction or covalent interaction. Fig. 1.2 depicts this idea in which the cube on the left has the same volume as the smaller cubes added together on the right. However, the total surface area is much larger for the smaller cubes.

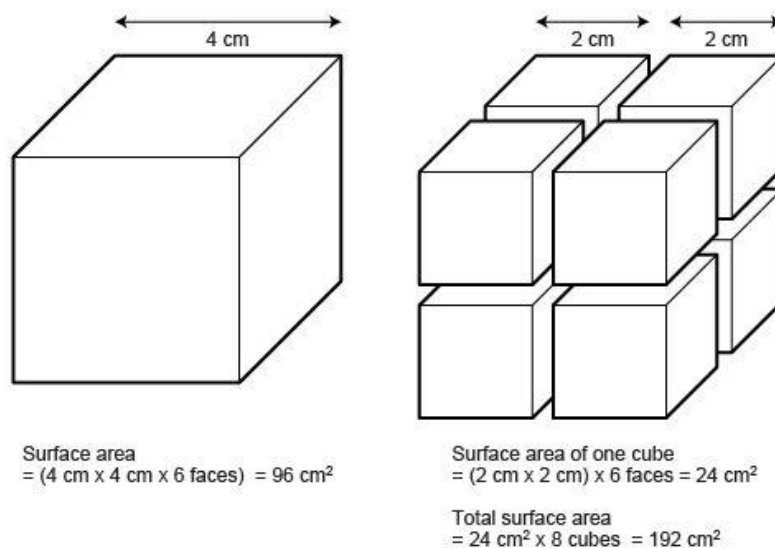


**Fig 1.2:** Increase in surface area as cube is cut into 8 pieces.

### 1.4 Methods of Generation of Nano-particles

Different methods of generation of nano-particles can be classified into two fundamental categories as shown in Fig 1.3. First category includes *bottom-up* or *build-up* approaches which begin with atoms and molecules at bottom level which react under certain chemical and physical circumstances to form nano-structures. Second category includes *top-down* or *break-down* approaches which begin with bulk material from top which is subsequently reduced into nano-structures by the way of physical, chemical and mechanical processes. Methods included in this category are also referred as *grain refining* methods in which surface energy of the particles increases which increases aggregation of the particles. Therefore, it is difficult to obtain particle sizes of less than 3 μm by grain refining because of

condensation of small particles also takes place simultaneously with pulverization. Grinding, mechanochemical methods and mechanical alloying are methods of nano-particles generation belong to this category. *Grinding* can be further sub-divided into two types namely wet grinding and dry grinding. In the *dry grinding* method the solid substance is ground by means of a shock, a compression, or by friction, using such popular methods as a jet mill, a hammer mill, a shearing mill, a roller mill, shock shearing mill, ball mill. On the other hand, *wet grinding* of a solid substrate is carried out using a tumbling ball mill, or a vibratory ball mill, a planetary ball mill, a centrifugal fluid mill, a flow conduit beads mill, or a wet jet mill. It is possible to obtain highly dispersed nano-particles by using wet grinding process because it can prevent condensation of the nano-particles so formed which is not possible with dry grinding.

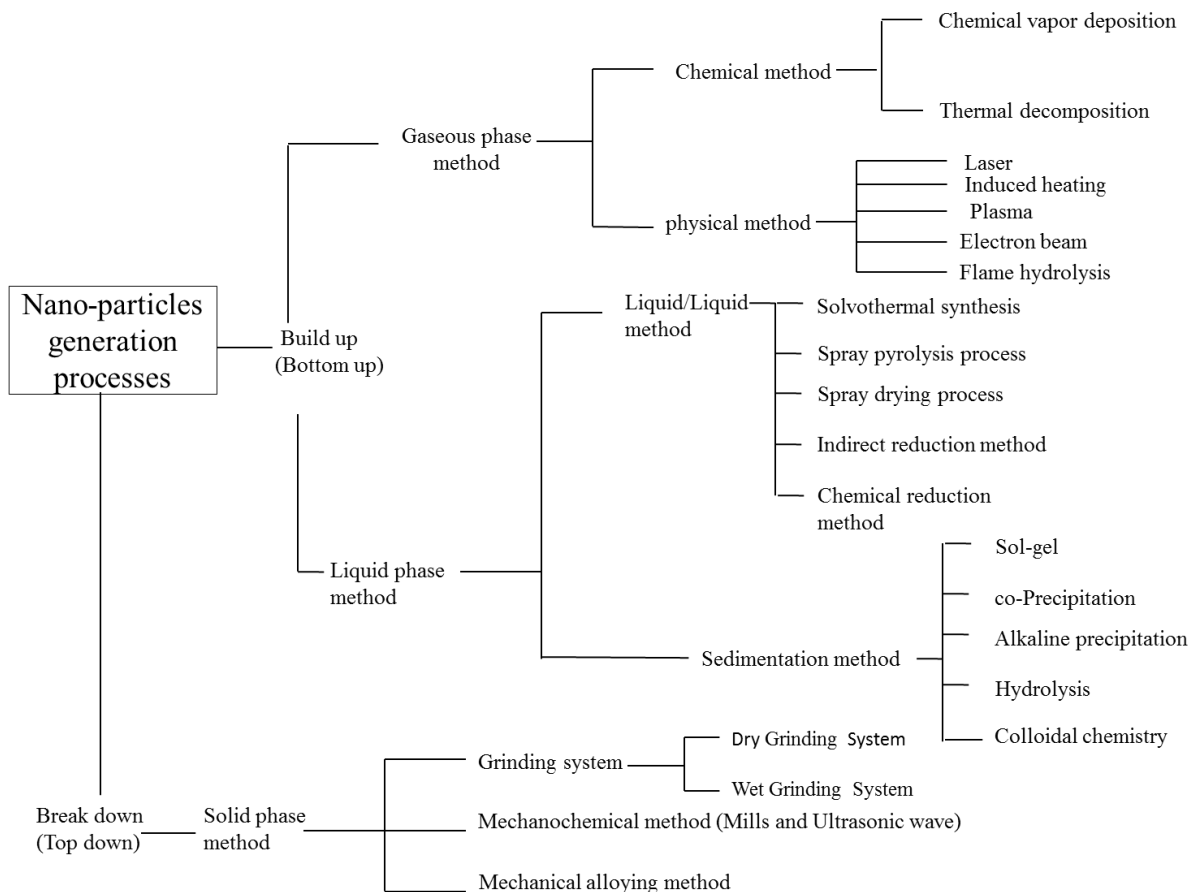


**Fig 1.3:** Different methods for generation of nano-particles.

The *bottom-up approaches* can be further divided into two groups namely (i) gaseous phase methods; and (ii) liquid phase methods. *Gaseous phase methods* include (a) chemical methods involving a chemical reaction such as chemical vapor deposition (CVD) and thermal deposition; and (b) physical vapor deposition (PVD) methods which involve evaporation of liquid or solid material using either laser, plasma, electron beam, induction heating or flame

hydrolysis and rapid cooling of the evaporated material yielding the desired nano-particles. *Liquid phase methods* have been the main methods for generation of nano-particles for many years. They can be further subdivided into two types i.e. (i) liquid/liquid methods: which include chemical reduction method, indirect reduction method, spray pyrolysis, spray drying and solvothermal synthesis; and (ii) sedimentation methods: which include sol-gel method, alkaline precipitation, co-precipitation, hydrolysis and colloidal chemistry method. The gaseous phase methods minimize the occurrence of organic impurities in the nano-particles as compared to the liquid phase methods but they necessitate use of complicated vacuum equipment whose disadvantages are the high costs involved and low productivity.

The *CVD* method can produce ultra-fine particles of size less than 1  $\mu\text{m}$  by the chemical reaction occurring in the gaseous phase. The manufacture of nano-particles of 10 to 100 nm is possible by careful control of the reaction. Performing the high temperature chemical reaction in the CVD method requires heat sources such as a chemical flame, a plasma process, a laser, or an electric furnace. *Thermal decomposition* method has been particularly useful in the production of metal oxide or other types of particles and has been used extensively as a preferred synthetic method in the industrial world. *Chemical reduction* of metal ions is a typical example of a liquid/ liquid method, whose principal advantage is the facile fabrication of particles of various shapes, such as nano-rods, nano-wires, nano-prisms, nano-plates, and hollow nano-particles. With this method, it is possible to fine-tune the form/shape and size of the nano-particles by changing the reducing agent, the dispersing agent, the reaction time and the temperature. It carries out chemical reduction of the metal ions to their 0 oxidation states. The process uses non-complicated equipment or instruments and can yield large quantities of nano-particles at a low cost in a short time.

*Sol-gel* method has been used extensively for the fabrication of metal oxide nano-particles. This procedure transforms a solution of a metal alkoxide into a sol by hydrolysis, followed by poly-condensation to a gel. The wet process (liquid phase method) guarantees a high dispersivity of nano-particles compared to the dry methods. However, if the resulting nano-particles are dried, aggregation of the particles soon follows. In this case, re-dispersion can be carried out according to the process used in the solid phase method.

There are some features that are common to all the methods of generation of nano-particles i.e. synthesis of nano-particles requires the use of a device or process that fulfills the following condition (**Horikoshi and Serpone, 2013**):

- ❖ Control of particle size, size distribution, shape, crystal structure, composition, distribution.

- ❖ Improvement in the purity of the nano-particles.
- ❖ Stabilization of physical properties, structures and reactants.
- ❖ Higher reproducibility and control of aggregation.
- ❖ Higher mass production, scale up and lower costs.

## 1.5 Applications of Copper Nano-particles

Among the various metallic and non-metallic nano-particles, synthesis of nano and ultra-fine particles of copper has attracted considerable attention because of their outstanding physical, chemical, catalytic, optical and electrical properties. Following are some worth-mentioning applications of copper nano-particles:

- ❖ Acts as an anti-biotic, anti-microbial and anti-fungal agent when added to plastics, coatings, and textiles
- ❖ Copper diet supplements with efficient delivery characteristics
- ❖ High strength metals and alloys
- ❖ Heat sinks and highly thermal conductive materials
- ❖ Efficient catalyst for chemical reactions and for the synthesis of methanol and glycol
- ❖ As sintering additives and capacitor materials
- ❖ Conductive inks and pastes containing copper nano-particles can be used as a substitute for very expensive noble materials used in printed electronics, displays, and transmissive conductive thin film applications
- ❖ Superficial conductive coating processing of metal and non-ferrous metal
- ❖ Production of multi-layer ceramic capacitor internal electrode and other electronic components in electronic slurry for the miniaturization of microelectronic devices
- ❖ As nano-metallic lubricant additives

## 1.6 Introduction to Electrochemical Dissolution Process

Electrochemical dissolution (ECD) process works on the principle of electrolysis which is governed by Faraday's laws of electrolysis which state that the (i) amount of chemical change produced by an electric current is directly proportional to the quantity of electricity passed; and (ii) amount of different substance dissolved or deposited by the *same* quantity of current are proportional to their chemical equivalent weight. Mathematically, Faraday's laws can be expressed as

$$m \propto E I t = \frac{E I t}{F} = \frac{M I t}{Z F}$$

Where,  $m$  is mass of the material being dissolved (grams);  $M$  is atomic weight of the material being dissolved;  $Z$  is valency of dissolution;  $t$  is time during which electrolysis is takes place (seconds);  $I$  is the amount of current passed (A);  $E$  is Electrochemical equivalent weight of the material being dissolved (grams); and  $F$  is Faraday's constant = 96,500 Coulomb.

ECD has been used for various applications in different industries such as automobiles, avionics, bio-medical, agriculture, defense equipment, electronic gadgets etc. since long time. Some typical applications of ECD and processes based on it are:

- ❖ Electroplating of electrically conductive materials
- ❖ Electrochemical machining of very complicated components and products made of hard-to-machine but electrically conducting materials
- ❖ Production of metals from metallic compounds to obtain the pure form of metal
- ❖ Production of electrolytic copper as a cathode from refined copper of lower purity as an anode
- ❖ Production of sodium chlorate and potassium chlorate
- ❖ Production of oxygen for spacecraft and nuclear submarines
- ❖ Production of hydrogen as fuel

But, very limited work has been done on generation of copper nano-particles by ECD process and use of pulsed-ECD has not been explored for same. Present work tries to bridge this gap.

### 1.6.1 Process Parameters of Pulsed-ECD

It is important to understand various process parameters of ECD and their importance during actual electrolysis process for nano-particle generation to understand the process behavior and exercise better control. Fig.1.4 illustrates various parameters of pulsed ECD using rectangular pulse and their effects on the nano-particle generation are described below.

- ❖ **Pulse-off Time ( $T_{off}$ ):** Duration in which current has minimum value which helps in maintaining the temperature of the electrolyte. Longer pulse-off time also helps in preventing the agglomeration of the nano-particles.
- ❖ **Peak Current ( $I_p$ ):** Peak current is the maximum value of pulsed current during pulse-on time.
- ❖ **Duty Cycle ( $T$ ):** It is ratio of pulse-on time to sum of pulse-on time and pulse-off time and is expressed as percentage i.e. it indicate the % duration in which peak current is maintained. Its value is determined by the heat sensitivity of the material and the

maximum current available from the power supply. Materials having higher thermal expansion may require a duty cycle on the peak current.

- ❖ **Pulse frequency ( $f$ ):** Pulse frequency is the number of pulses per second. One pulse consists of one pulse-on and the adjacent pulse-off time.

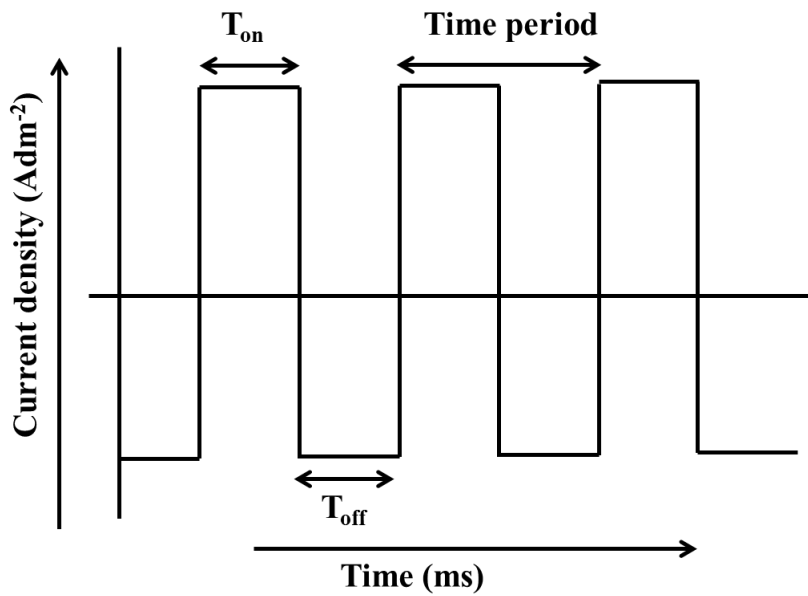


**Fig 1.4:** Schematic representation of rectangular pulse in PECD process.

*Next chapter* presents review of past work on nano-particles synthesis using different processes, research gaps identified based on this review, the research objectives defined based on the identified research gaps and research methodology used in the present work.



## Chapter 2

### Review of Past Work and Research Objectives

Various methods have been used for generation of nano-particle namely ball milling, micro electric discharge machining ( $\mu$ -EDM), flame combustion synthesis, laser ablation, wire explosion, sol-gel etc. Each process has some advantages and limitation. Table 2.1 presents summary of type of energy, material applications, limitations and advantages of these methods .

**Table 2.1:** Summary of material applications, limitations, advantages of different methods of nano-particles generation used in past.

| Processes              | Type of energy used | Material applications   | Limitations   | Advantages  |
|------------------------|---------------------|---|---|---|
| Micro-EDM              | Thermal Energy      | Electrically conductive material i.e. aluminum, Copper                  | Some Inert gas and inorganic impurities.                            | Low cost and high production rates                    |
| Laser ablation         | Thermal Energy      | Metal, organic, solids, Semiconductors i.e. gold, copper                | The ablation of target in gaseous flow gives access to airborne NPs | Simple, reliable and chemically pure Nano material    |
| Wire explosion         | Thermal Energy      | Thin metal, conductors i.e. tungsten, aluminum, copper.                 | Inert gas impurities due to inert atmosphere.                       | Purity of powder produced by wire explosion is high.  |
| Electric arc discharge | Thermal Energy      | Metal and metal containing i.e. aluminum                                | Oxide formation example: formation of Nano alumina in making of Al  | Cost effective and flexible process for metallic NPs  |
| Sol-Gel process        | chemical energy     | Ceramics i.e. silica, titanium oxide, glass                             | Oxide formation   | Low temperature technique and generate small size NPs |
| Flame combustion       | Thermal Energy      | Generally metal and metal oxide i.e. titanium oxide, silver, palladium. | Oxide formation   | Mono disperse particle formation                      |

*Ball milling* has been used to generate nano-particles of metals and ceramics i.e. carbon and boron tube. It uses kinetic and potential energy and is a very fast process. But, particle

generated by this process are observed to be contaminated by milling tool and the ambient atmosphere. *Micro-EDM* has been used for generating nano-particles of electrically conductive material but oxide formation is the main drawback of this process. *Laser ablation* has been used for generation of nano-particles of metals, semiconductors, organic materials. This process has capability to generate pure nano-particles and it is simple, fast and reliable process but the ablation of target in gaseous flow gives access to airborne nano-particles. *Wire explosion* utilizes thermal energy to generate nano-particles and it can generate nano-particles of metallic conductors i.e. tungsten, aluminum, copper. High purity nano-powder is obtained through this process but this process has a drawback of impurities due to inert gas atmosphere. *Flame combustion* has been used for generating nano-particles of metal and metal oxides such as tungsten, aluminum, copper. Mono-dispersed particles can be synthesized by this process but has a drawback of oxide formation. *Electric arc discharge* process has been used for generating nano-particles of metal and metal containing materials i.e. titanium oxide, silver, palladium. The only drawback is oxide formation. ECD process has potential to overcome above-mentioned disadvantages of various processes of nano-particle generation. It has capability to generate uniform size and pure nano-particles.

## 2.1 Review of Past Work on Generation of Nano-particles

Table 2.2 present summary of past work done on generation of nano-particles of different materials using different methods. Following paragraphs describe them briefly:

**Table 2.2:** Summary of past work on generation of nano-particles.

| Processes        | Researchers (year)                              | Material       | Size of particles |
|------------------|---|----------------|-------------------|
| Micro-EDM        | <b>Sahu <i>et al.</i> (2014a)</b>               | Aluminum       | 90 nm             |
|                  | <b>Sahu <i>et al.</i> (2014b)</b>               | Copper         | >10 nm            |
| Wire             | <b>Sarhi <i>et al.</i> (2008)</b>               | Tungsten       | 10 to 150 nm      |
| Explosion        | <b>Wankhede <i>et al.</i> (2013)</b>            | Copper         | 10 to 100 nm      |
| Laser ablation   | <b>Boutinguiza <i>et al.</i> (2013)</b>         | Titanium oxide | 5 to 25 nm        |
| Flame combustion | <b>Ma <i>et al.</i> (2014)</b>                  | Titania        | 80 to 120 nm      |
| Electric arc     | <b>Yanık <i>et al.</i> (2013)</b>               | Aluminum       | 51 nm             |
| Ball milling     | <b>Rajesh Kanna and Nirmal kumar (2014)</b>     | Copper         | 100 to 200 nm     |
| ECD              | <b>Nekouei <i>et al.</i> (2013a-2013c)</b>      | Copper         | 200 nm            |
|                  | <b>Theivasanthi and Alagar (2011)</b>           | Copper         | 24 nm             |
|                  | <b>Maksimović <i>et al.</i> (2009a, 2009b)</b>  | Copper         | > 50 microns      |
|                  | <b>Theivasanthi and Alagar (2012)</b>           | Silver         | 24 nm             |
|                  | <b>Rodri'guez-Sa'nchez <i>et al.</i> (2000)</b> | Silver         | 2 to 7 nm         |

**Sahu et al. (2014a)** used  $\mu$ -EDM process to generate nano-particles of *aluminum*. This was performed with various operating parameter such as current, voltage, pulse duration, duty cycle. TEM study showed that size of aluminum nano-particles dispersed in deionized (DI) water lies in the range of 50-130 nm with average primary (nano-aluminum clusters) size of approximately 90 nm. The mean size of aluminum particle through dynamic scattering study was found to be 260 nm with geometric deviation of 1.68. The size distribution of generated aluminum nano-particles indicates narrow distribution. **Same authors (2014)** used  $\mu$ -EDM to generate and characterize nano-particles of *copper*. In this study an innovative approach was made for generation of copper nano-particles using the developed micro-EDM process in both DI water and DI water with PVA (polyvinyl alcohol) and PEG (polyethylene glycol) stabilizing agents. The TEM study showed that the size range of copper nano-particles dispersed in pure DI water was in the range of 600–1100 nm, with PVA sample in the range of 2–10 nm and with PEG sample in between 4–10 nm. The size distribution study of generated copper nano-particles showed that the measurement follows normal distribution with mean size being less than 10 nm.

**Sarathi et al. (2008)** used *wire explosion* process to generate and characterize *tungsten* nano-particles. The impact of ambient medium on the size of the produced particles was examined. Cooling rate of the particles was high in helium atmosphere leading to high saturation ratio. Mean size of the particles was less in helium atmosphere confirming the influence of cooling rate on the particle size. The TEM study showed that the produced tungsten particles were of spherical shape. Study of particle size distribution indicated that it follows log-normal probability distribution. The EDAX results showed that presence of oxygen and nitrogen contents was very less in the produced powder, indicating the purity of the powder produced by wire explosion process. **Wankhede et al. (2013)** also used wire explosion process for the synthesis *copper* nano-particle synthesis by wire explosion process. In their apparatus, increase in energy reduced the particle size and increase in wire diameter of copper reduced the particle size. No linear relation between these parameters existed. Range of particles size was observed to be 10-100 nm by analysis done using field emission scanning electron microscopy. Higher energy with the lower wire diameter should be preferred for finer size nano-particles. This process required less than 100  $\mu$ -sec for production of nano-particles indicating higher production rate.

**Boutinguiza et al. (2013)** used Ytterbium fiber *laser ablation* to generate *titanium oxide* nano-particles. They ablated particles in de-ionized water and in ethanol and produced stable colloids of titanium oxides. The nano-particles were formed as result of the reaction between

the melted metal and oxygen from the vaporized solvent to give titanium oxide. They observed morphology of the particles as almost perfect sphere, and in all experiments TEM images of the particles exhibited the same perfect rounded appearance. The size of the particles was found to be in the range of 5 to 25 nm. Despite the presence of some occasional large particles, the particle size distribution was quite narrow. **Kumar et al. (2014)** used *laser ablation* to generate **copper** nano-particles in different liquids i.e. aqueous solution of sodium dodecyl sulfate, acetone and ethanol from a bulk copper target using 1,064 nm from Nd: YAG laser. Transmission electron microscopy and UV–vis spectrometry was employed for the analysis of size and optical properties of the nano-particles, respectively. X-ray diffraction patterns confirmed formation of copper nano-particles. The nano-particles exhibit hexagonal nature with average particle size of 15–25 and 20–30 nm in case of sodium dodecyl sulfate and acetone respectively, whereas they possess spherical symmetry with bigger particle size of 30–40 nm in ethanol.

**Ma et al. (2014)** used *flame combustion* process to synthesize **titania** (TiO<sub>2</sub>) and reported formation mechanism of nano-particles. They have built a mono disperse particle formation model (MPF) and five-zone diagram (FZ diagram) was used to examine the titania combustion synthesis process. Results of the FZ diagram as well as particle size were investigated via three parameters in the MPF model: particle number density (N), total aggregate volume per unit mass of gas (V) and total aggregate surface area per unit mass of gas (A). Change in the ratio of inlet oxygen/nitrogen from 20/80 to 50/50 enhanced the high temperature zone, which increased the collective particle sizes from 81.4 to 120.9 nm.

**Yanık et al. (2013)** used *electric arc discharge* to generate and characterize **aluminum** nano-particles by electric arc technique. Aluminum nano-particles were prepared by arc discharging at different applied current in the range of 65–90A and arc media consisting of distilled water and ethylene glycol. The density of applied current and media has profound impact on particle size, morphology and chemical composition of synthesized aluminum nano-particles. It was observed that decrease in applied current results in a decrease in particle size. Ethylene glycol as media provided the highest purity, most dispersed and relatively smallest size of aluminum nano-particles. Average particle size was found to be 51 nm in ethylene glycol and 66 nm in distilled water at 65A.

**Akbar et al. (2004)** used *sol-gel* method and investigated the structural and magnetic characteristics of nano-particles of **ferric oxide** (Fe<sub>2</sub>O<sub>3</sub>) of different sizes obtained in range from 22 to 56 nm. Pure alpha phase particles as well as particles with a mixture of alpha and gamma phase were obtained and identified by x-ray. The average size of the particles

decreased with increased annealing temperature of the gel and with the increase in the concentrations of the citric acid. The annealing temperature affects the relative fractions of the two phases and consequently the magnetization of the particles.

**Rajeshkanna and Nirmalkumar (2014)** used high energy *ball milling* process to generate and characterize *copper* nano-particles which were found to be spherical in shape. Powder samples have been taken by high energy ball milling (HEBM) at 30 hrs, 45 hrs and 75 hrs and constant speed of 250 rpm with the ball to powder mass ratio (BPR) 10:1. The average particle size was observed to be 200 nm at 30 hr; 100 nm at 50 hr and 100 nm at 75 hr.

**Nekouei et al. (2013a)** used *electrolysis* process to generate *copper* nano-particles in sulfate and nitrate solution. The use of pulse current has a positive effect on the reduction of particle size in the copper powder synthesis in sulfate solution, but this effect was not very significant. Sulfate solution along with additives reduces the particle size to less than 200 nm. However, in nitrate solution, spherical particles were well synthesized to size less than 100 nm. Efficiency of the nitrate solution was very low (about 30%). The produced powder was of very high purity. An increase in the nitric acid concentration from 25 to 45g/L resulted in small changes in the particle size. Change of type of the current from direct to pulse in the nitrate solution leads to severe agglomeration of the powder; generation of disk morphology; and severe reduction in the current efficiency. Pulse current in the nitrate solution (at least under the tested conditions) did not produce *nano-powders*. Same authors (2013c) used concept of design of experiment to synthesize ultra-fine *copper* particles by *electrolysis* process. A mathematical model was proposed by analysis of variance. They studied effects of four parameters namely current density, sulfuric acid concentration, copper ion concentration and chloride ion concentration, on the process performance. They found particle size at the optimum condition as 0.71  $\mu\text{m}$  which was very close to the experimental value of 0.68  $\mu\text{m}$ .

**Theivasanthi and Alagar (2011 and 2012)** used *electrochemical dissolution* process to characterize and synthesize nano-particles of *copper* and *silver*. They used XRD, SEM and Fourier transform infrared spectroscopy (FTIR) spectroscopic techniques to characterize the nano-particles and found that the produced particles were in spherical shape having size of 24 nm. Investigation on the antibacterial effect of nano-sized copper against E. coli and B. megaterium microbes revealed high efficiency of copper nano-particles as a strong antibacterial agent. Specific surface area (SSA) of copper nano-particles prepared in two different methods have been analyzed which concludes that increased SSA results in the enhancement of antibacterial activities of copper nano-particles. Likewise, analysis results of

SSA of two different bacteria concluded that SSA of bacteria plays a major role while reacting with antimicrobial agents.

**Rodri'guez-Sa'nchez et al. (2000)** used *electrochemical dissolution* for the synthesis of *silver* nano-particles by reduction of anodically solved silver ions in acetonitrile containing tetrabutylammoniumsalts (TBA bromide or TBA acetate). They obtained particle size in the range of 2 to 7 nm. Silver nano-particles obtained studied. They found that current density plays an important role, not only in determining the particle size but also the efficiency of the process. The cathode nature seemed to be also a decisive parameter, because only particles obtained when platinum instead of aluminum was employed. The spectra of silver sols showed the presence of two different silver clusters. The smallest clusters were present from the beginning to the end of the process, and this suggested that clusters were continuously generated.

## 2.2 Identified Research Gaps

Following research gaps were identified from the review of past work:

- ❖ Ball milling, wire explosions, micro-EDM, laser ablation, electric arc discharge, flame combustion, sol-gel processes have been used to generate nano-particles of different materials.
- ❖ Very limited work has been done for generation of nano-particles by ECD.
- ❖ No work has been done on generation of nano-particles of copper using pulsed electrochemical dissolution (PECD) process and to study effect of concentration, time, inter electrode gap, voltage, pulse-on time and pulse-off time on size and shape of copper nano-particles.

## 2.3 Research Objectives of the Present Work

Following research objectives were identified on the basis of the review of the past work and the identified research gaps:

- ❖ To generate nano-particles of copper by pulsed electrochemical dissolution (PECD) process i.e. machining products during ECM process.
- ❖ Design and development of the electrolytic cell for the same
- ❖ Design and fabrication of suitable cathode
- ❖ Selection of appropriate electrolyte and its parameters such as type, composition, concentration, flow rate and temperature
- ❖ Selecting appropriate method for collecting nano-particles generated by PECD

- ❖ Experimental Investigations on effect of different PECD parameters on morphology and chemical composition of the generated copper nano-particles.
- ❖ To identify optimum PECD parameters to generate best morphology copper nano-particles.

## 2.4 Research Methodology

Figure 2.1 depicts the research methodology used in the present work to meet the identified research objectives. The experimental research in the present work was planned and conducted in two stages: (i) *pilot experiments* to study the effect of electrolyte concentration, inter electrode gap (IEG) and time on the nano-particles shape and size using Box-Behnken approach of response surface methodology (RSM) and identify their optimum combination for further experiments; (ii) *main experiments* to study the effects of pulse-on time, pulse-off time overall influence of input process parameters on the process performance using central composite approach of RSM .

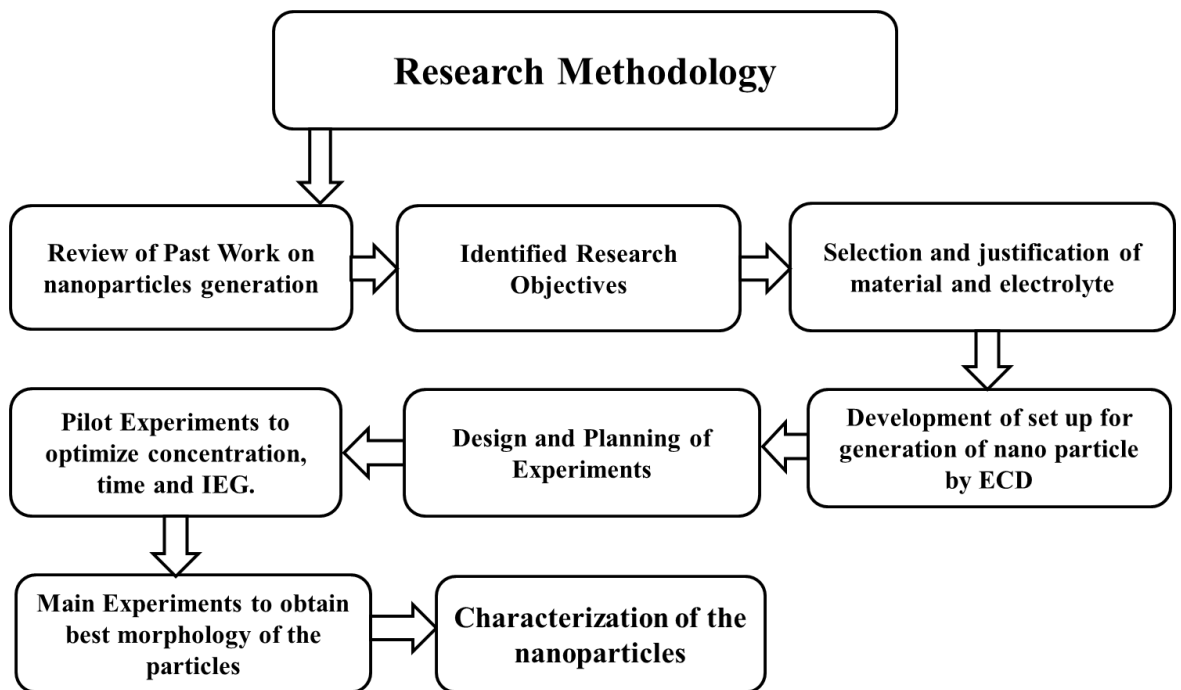


**Fig 2.1:** Research methodology used in the present work.

*Next chapter* presents the fabrication of the experimental apparatus, different sub-systems and the components used in the development of the experimental apparatus and working of the experimental apparatus.



## Chapter 3

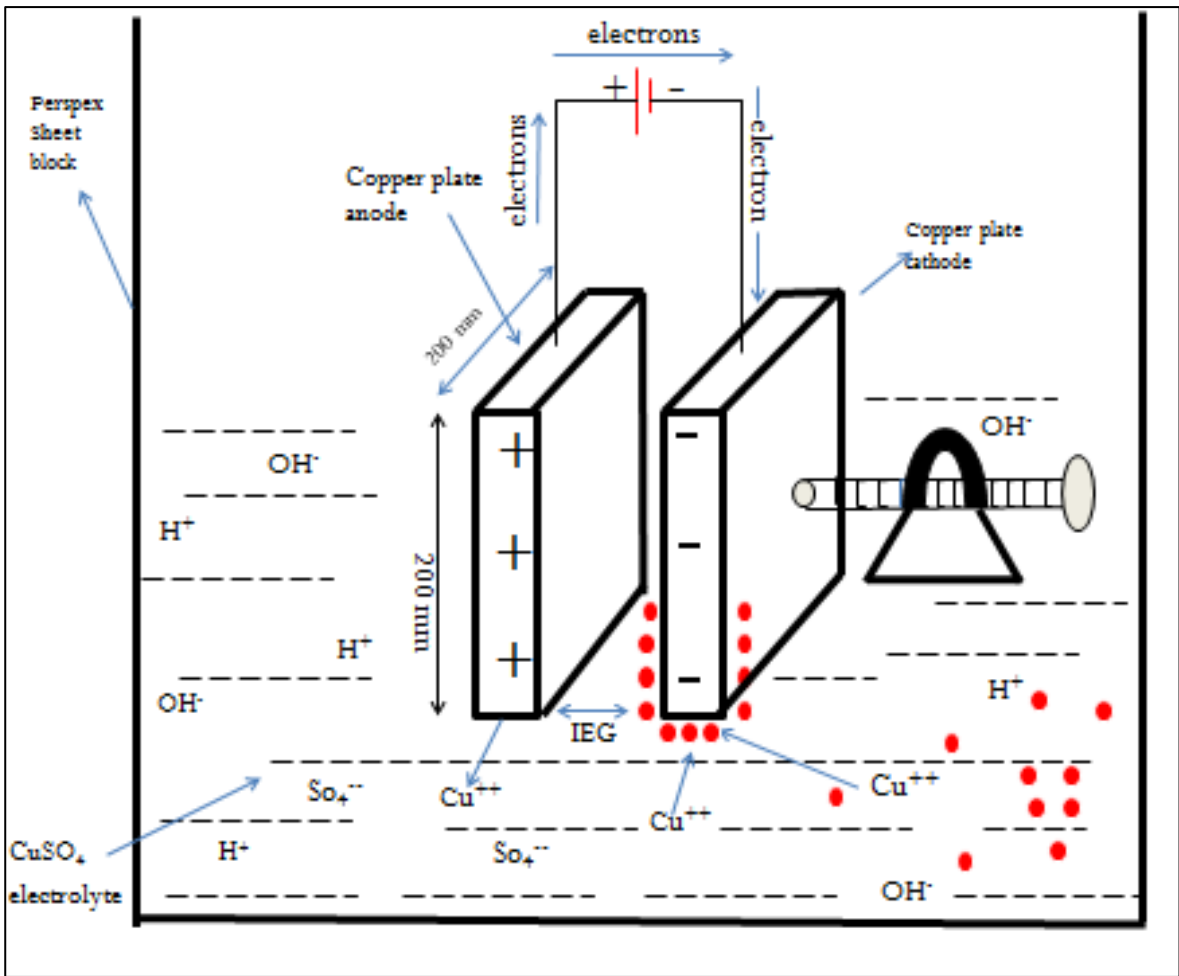
### Development of Experimental Apparatus

This chapter presents details of development and working of the experimental apparatus used for generation of copper nano-particles by PECD process.

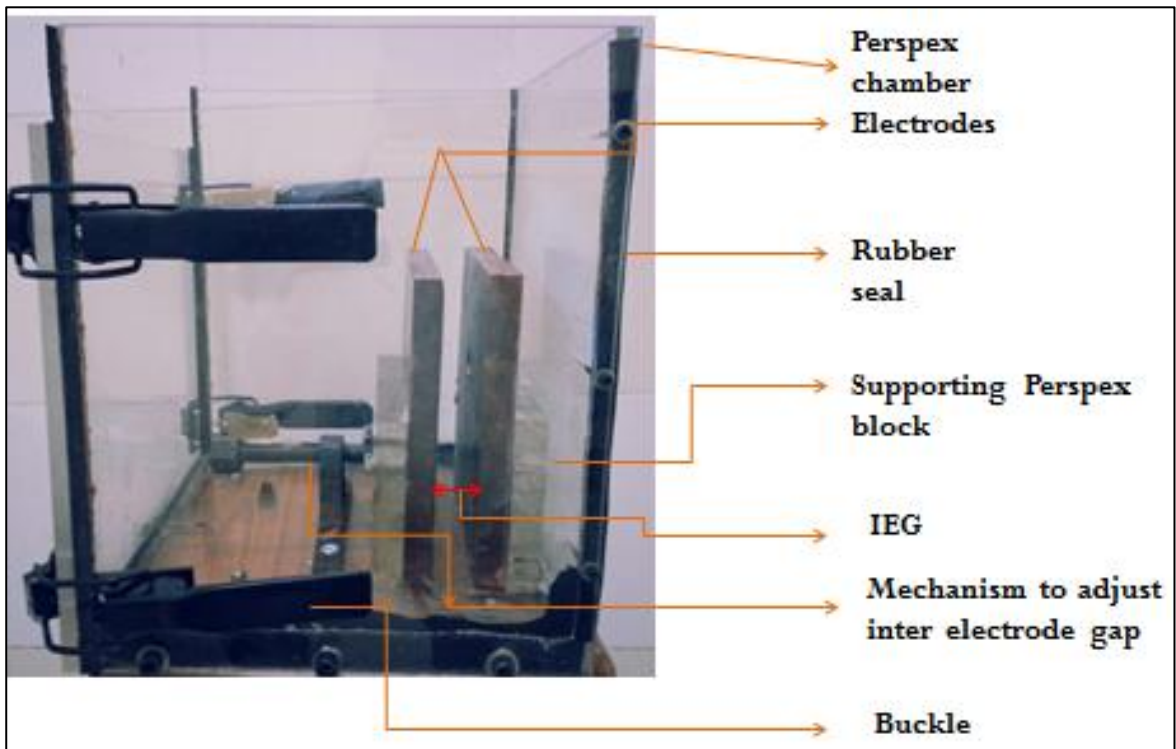
#### 3.1 Development and Working of Experimental Apparatus

Figure 3.1 depicts schematic and photograph of the experimental apparatus developed for the generation of nano-particle by PECD. The apparatus consists of four systems: (i) Power supply; (ii) Electrodes; (iii) Mechanism to adjust inter electrode gap (IEG); and (iv) Housing. The apparatus has two electrodes both made of copper. The positive terminal of DC pulsed power supply was connected to first copper electrode to make it anode while the negative terminal was connected to second electrode to make it cathode. These two electrodes were submerged in copper sulphate electrolyte. A threaded screw with supporting clip was used to adjust the inter-electrode gap. The whole apparatus was enclosed in a housing made of perspex sheets.

**Working principle of electrolytic dissolution process:** Whenever copper sulfate ( $\text{CuSO}_4$ ) is added to water, it gets dissolved in the water. As the  $\text{CuSO}_4$  is an electrolyte, it splits into  $\text{Cu}^{++}$  (cation) and  $\text{SO}_4^{--}$  (anion) ions and move freely in the solution. Now, if two copper electrodes are immersed in that solution, the  $\text{Cu}^{++}$  ions (cation) will be attracted towards cathode i.e. the electrode connected to the negative terminal of the power supply. On reaching on the cathode, each  $\text{Cu}^{++}$  ion will take electrons from it and becomes neutral copper atoms. Similarly, the  $\text{SO}_4^{--}$  (anion) ions will be attracted by anode i.e. the electrode connected to the positive terminal of the power supply. So,  $\text{SO}_4^{--}$  ions will move towards anode where they give up two electrons and become  $\text{SO}_4$  radical but since  $\text{SO}_4$  radical cannot exist in the electrical neutral state, it will attack copper anode and will form copper sulfate. This process is called electrolysis. After taking electrons the neutral copper atoms get deposited on the cathode. At the same time,  $\text{SO}_4$  reacts with copper anode and becomes  $\text{CuSO}_4$  but in water it cannot exist as single molecules instead of that  $\text{CuSO}_4$  will split into  $\text{Cu}^{++}$ ,  $\text{SO}_4^{--}$  and dissolve in water. So, it can be concluded that during electrolysis of copper sulfate with copper electrodes as shown in Fig 3.1, copper is deposited on cathode and same amount of copper is removed from anode.



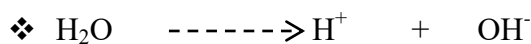
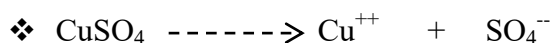
(a)



(b)

**Figure 3.1:** The developed experimental apparatus: (a) schematic diagram; (b) photograph.

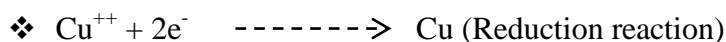
**Chemical Reactions:** When copper sulphate is dissolved in water, following reaction will occur



At anode, following reaction will occur



At cathode, following reaction will occur



### 3.1.1 Power Supply Unit

A computer controlled DC power supply unit (model 3300 W DC power supply) was used to supply pulsed DC power supply current in the IEG. The unit has capability of supplying an output voltage in the range of 0-100 V for low voltage units and 0-660 V for high voltage application, current in the range of 10-110 A and computer controlled programmable options for setting pulse-on time and pulse-off time. Fig 3.2 shows the photograph of pulse power supply.



**Figure 3.2:** Photograph of the pulsed DC power supply unit.

The unit can provide both pure DC and pulse power supply by changing the option in the power supply. It has programmable sequencer to use as an arbitrary waveform generator and create loops ramps and the sequencer is controlled via Ethernet programming. So this system offers dual process capability for electrolytic dissolution process (pure DC and pulse power supply). It provides flexibility for selecting best suitable parameters as per the requirement of the process. An oscilloscope is a type of electronic test instrument that allows observation of constantly varying signal voltages, usually as a two-dimensional plot of one or more signals as a function of time. Other signals (such as sound or vibration) can be converted to voltages and displayed. It shows the values of rise and fall time which reveals the actual time taken in the electrolysis. Fig 3.3 shows the photograph of oscilloscope.

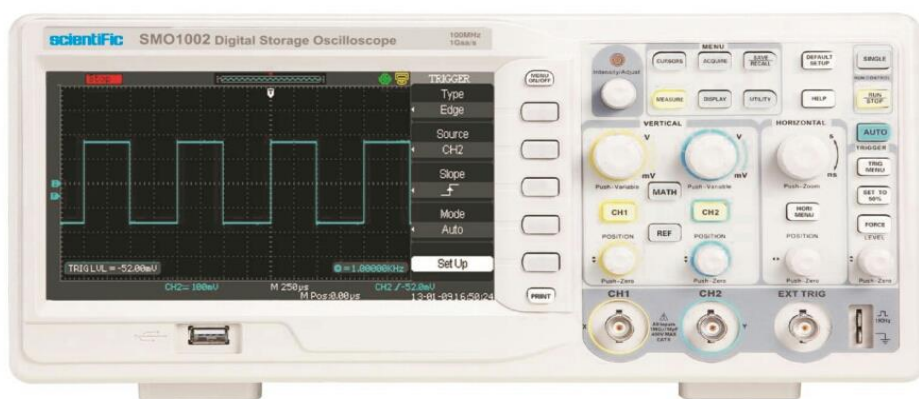


**Figure 3.3:** Photograph of the oscilloscope

### 3.1.2 Electrodes

Two copper plates were used for fabricating both the cathode and anode. Size of the copper plate chosen was 200 x 200 x 20 mm. Rectangular configuration of copper plates was chosen because it will remove material only from one side (unlike in case of cylindrical shape, material removal will take place uniformly) that will help to do more number of experiments without replacing the electrodes and easily hold on to the base of electrolyte cell as compared to cylindrical shape. Large size of copper plates (200 x 200 x 20 mm) was chosen because more number of experiments can be performed and it will save apparatus time in replacement of new electrode.

### 3.1.3 Mechanism for Adjusting Inter-electrode Gap

It is very essential to change the inter-electrode gap (IEG) because it affects the material removal rate. More the IEG, lesser will be material removal rate (MRR) and fewer particles will be formed and vice versa. So, IEG is an important parameter for the nano-particle generation by PECD process. Fig 3.4 shows the mechanism used to adjust the IEG in the present work. As shown in fig. one mechanism is fabricated to adjust the inter electrode gap.

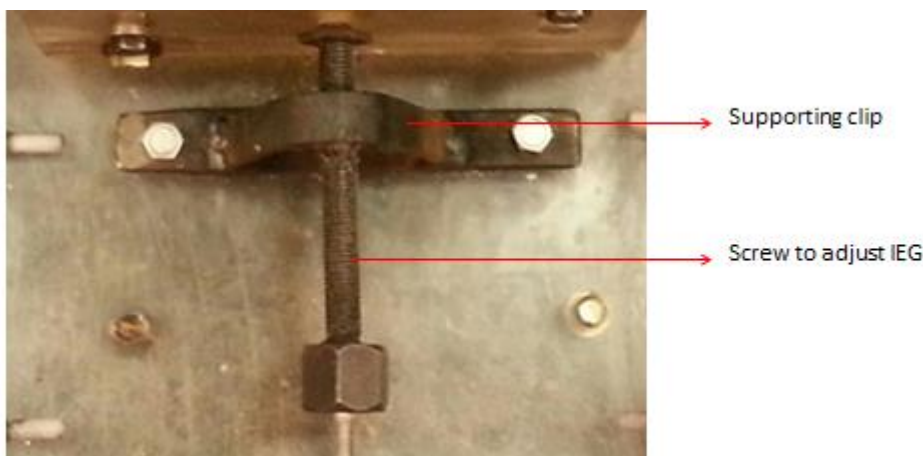


**Figure 3.4:** Photograph of the mechanism to adjust the IEG.

### 3.1.4 Housing of Experimental Apparatus

Electrodes are enclosed in a housing chamber made of perspex sheets of dimensions 350mm x 350mm for better visibility, corrosion-resistance and better strength-to-weight ratio. Fabricated chamber also has provisions for supply of fresh electrolytes, for removal of used electrolyte, and for escape of gases generated during the electrolytic process. Rubber seal was used for preventing of water leakage from the apparatus. It makes the apparatus water leak proof. Buckles are used for easily opening and closing of door. .

### 3.2 Selection of Material for Electrodes

Copper was selected for electrodes because

- ❖ Copper particles has wide range of application in heat transfer systems, antimicrobial material, super strong material, sensors and catalysts
- ❖ Copper is less costly as compared to noble materials and easily available.
- ❖ Copper has very high electrical conductivity making it suitable for electrochemical dissolution process

### 3.3 Selection of Electrolyte

Main function of electrolyte in the PECD is to perform electrochemical functions. Desirable properties of electrolyte include: high electrical conductivity, low viscosity, high specific heat, chemical stability, non-corrosiveness, non-toxic, low cost, and easy availability. Copper sulfate was selected as electrolyte because

- ❖ Provide copper ions so the ions in the electrolytic bath are continuously replenished by the anode
- ❖ Strong electrolyte so produce more ions in the solution
- ❖ Easily available

*Next chapter* describes planning and details of experiments carried out for the present work. It presents the planning and designing of pilot and main experiment.



## Chapter 4

### Planning of Experimental Investigations

Experimental investigations were carried out to ascertain the relationship between input parameters and measures of process performance. It avails to study the effect of different parameters on the morphology of the copper nano-particles. Experimental investigations were carried out in two phases: pilot experiment and main experiments to identify optimum combination of important PECD parameters for generation of copper nano-particles.

#### 4.1 Planning of Pilot Experiments

Pilot experiments were conducted to study the effect of electrolyte concentration, inter electrode gap (IEG) and time on shape and size of the nano-particles and to identify their optimum combination for the main experiments. Applied DC voltage, pulse-on time and pulse-off time were kept constant during these experiments whose values were selected keeping in the process principle of PECD and past work. Fifteenth pilot experiments were designed according to Box-Behnken Design (BBD) of experiment approach of response surface methodology (RSM) in which electrolyte concentration, IEG and time were varied at three levels each. Table 4.1 presents details of variable and fixed parameters, their selection criteria and responses used in the pilot experiments.

**Table 4.1:** Details of variable and fixed parameters, their selection criteria and responses used in the pilot experiments.

| <b>Variable parameters<br/>(Selection criteria)</b>                                      | <b>Fixed parameters<br/>(selection criteria)</b>                       | <b>Responses</b>  |
|--|--|---|
| 1. Electrolyte concentration (wt. %):<br>5, 7.5, 10<br>(Process principle and past work) | 1. Electrolyte: CuSO <sub>4</sub><br>(Process principle and past work) | 1. Surface morphology<br>using SEM images                   |
| 2. Time: 15, 30, 45 minutes<br>(Process principle and past work)                         | 2. Voltage: 12 V<br>(Process principle and past work)                  | 2. Chemical composition<br>using X-ray diffraction<br>(XRD) |
| 3. IEG: 5, 10, 15 mm<br>(Process principle)  | 3. Pulse-on time: 2 ms<br>(Process principle)                          |   |
|  | 4. Pulse-off time: 4 ms<br>(Process principle)                         |   |

Box-Behnken design is an independent quadratic design in that it does not contain an embedded factorial or fractional factorial design. In this design the treatment combinations are at the midpoints of edges of the process space and at the center. These designs are rotatable (or near rotatable) and require 3 levels of each factor. The designs have limited

capability for orthogonal blocking compared to the central composite designs. Fig 4.1 shows the Box-Behnken Design for three parameters to be varied at three levels each.

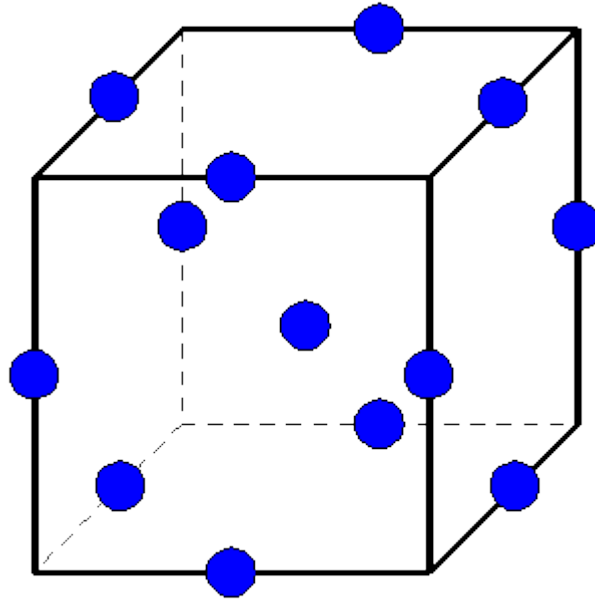


**Fig 4.1:** Box-Behnken experimental design for three parameters varying at three levels each.

## 4.2 Planning of Main Experiments

Main experiments were conducted to study influence of voltage, pulse-on time and pulse-off time on shape and size of the nano-particles and to identify their optimum combination for best morphology copper nano-particles. Electrolyte concentration, IEG and time were kept constant during these experiments at the optimum values identified from the pilot experiments. Twenty seven main experiments were designed and conducted using full factorial approach varying voltage, pulse-on and pulse-off time at three levels each. Table 4.2 presents details of variable and fixed parameters, their selection criteria and responses used in the main experiments.

**Table 4.2:** Details of variable and fixed parameters and responses used in the main experiments.

| Variable parameters<br>(Based on the past work) | Fixed parameters (identified<br>from the pilot experiments) | Responses               |
|---|---|-------------------------|
| 1. Voltage (V): 8, 12, 16                       | 1. Electrolyte Type: CuSO <sub>4</sub>                      | 1. Surface morphology   |
| 2. Pulse-on time (ms): 2, 4, 6                  | 2. Electrolyte concentration: 5 %                           | using SEM images        |
| 3. Pulse-off time (ms): 4, 8, 12                | (by weight)   |                         |
|   | 3. Time : 15 min  | 2. Chemical composition |
|   | 4. Inter Electrode Gap: 10 mm.                              | using XRD and EDX       |

### 4.3 Characterization of Nano-particles

Shape and size of the copper nano-particles generated in pilot and main experiments were determined using scanning electron microscopy (SEM) images. Chemical composition of the copper nano-particles having good morphology was determined using X-ray diffraction (XRD) and energy-dispersive X-ray spectroscopy (EDX).

### 4.4: Procedure of Experimentation

Fig 4.2 shows the procedure to generate nano-particles by ECD

#### Procedure to generate Nano-particles by ECD

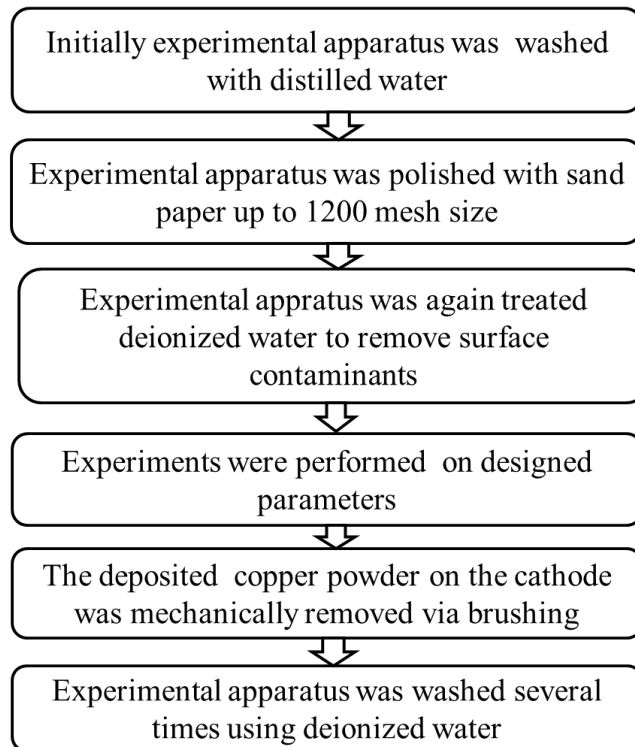


**Fig 4.2:** Procedure to generate nano-particles by ECD

*Next chapter* presents results of pilot and main experiments and their analyses focusing on the effects of variable parameters on shape and size of the copper nano-particles with an objective to identify the optimum combination of the PECD process parameters. It also presents SEM images, results of XRD and EDX and their analysis.



## Chapter 5

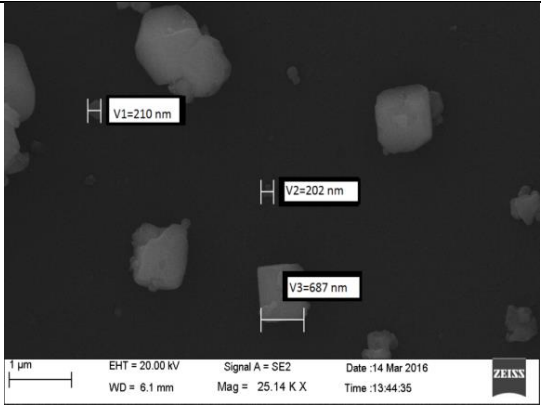
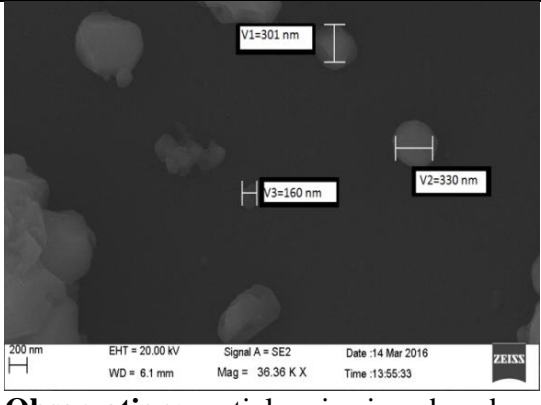
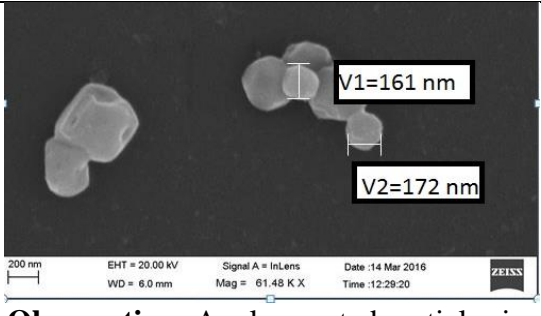
### Results and Discussion

This chapter presents results of pilot and main experiments, characterization of copper nano-particles by SEM images, determination of their chemical composition by EDX and XRD. It also describes the effects of variable parameters of pilot and main experiments on average size and shape of the generated copper nano-particles. The results have been analyzed to identify that optimum combination of electrolyte concentration, IEG and time from the pilot experiments and optimum combination of voltage, pulse-on time and pulse-off time from the main experiments, which will give optimum morphology of the copper nano-particles. Chemical composition of copper nano-particles has been analyzed for the optimum morphology copper nano-particles.

#### 5.1 Pilot Experiments

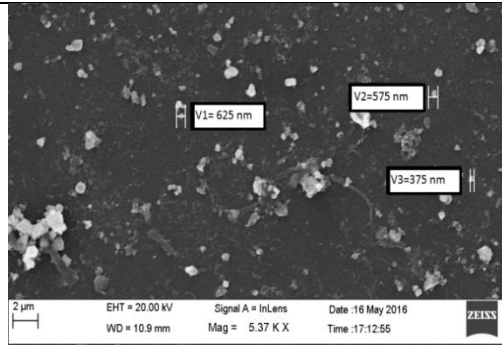
Table 5.1 presents input parameters, average size of the generated copper nano-particles along with their SEM images for different 15 runs of the pilot experiments. It can be observed from table 5.1 that the minimum value of average size of the generated copper nano-particles (150 nm) is obtained for electrolyte concentration as 5 wt. %, inter electrode gap as 10 mm and operating time as 30 minutes.

**Table 5.1:** Average size of the generated copper nano-particles and their SEM images for different input parameters combinations in 15 pilot experiments.

| Exp. No. | Electrolyte concentration (wt.%) | IEG (mm) | Time (minutes) | Avg. size of Cu nano-particles (nm) | SEM image, observations and conclusions   |
|----------|----------------------------------|----------|----------------|-------------------------------------|---|
| 1        | 7.5                              | 15       | 15             | 530                                 |  <p><b>Observation:</b> Some particles are found to be in rectangular shape. Large size particles is formed</p> <p><b>Conclusion:</b> Due to high concentration</p> |
| 2        | 5                                | 15       | 30             | 170                                 |  <p><b>Observation:</b> particles size is reduced</p> <p><b>Conclusion:</b> Due to lower concentration and optimum time</p>  |
| 3        | 5                                | 5        | 30             | 165                                 |  <p><b>Observation:</b> Agglomerated particles is formed</p> <p><b>Conclusions:</b> Due to less IEG</p>   |

---

4      7.5      10      15      525

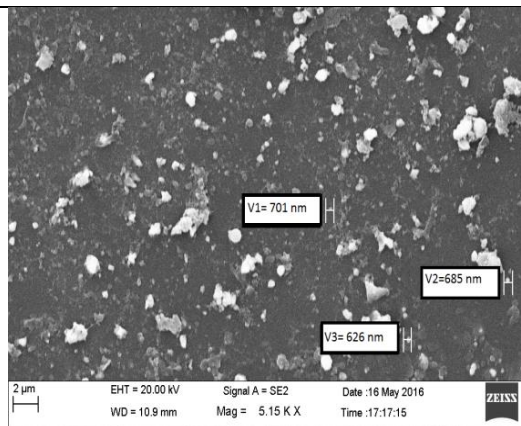


**Observation:** Particles are irregular in shape. Agglomerated and mono dispersed particles are found at different places.

**Conclusion:** due to high electrolyte concentration

---

5      10      10      45      680

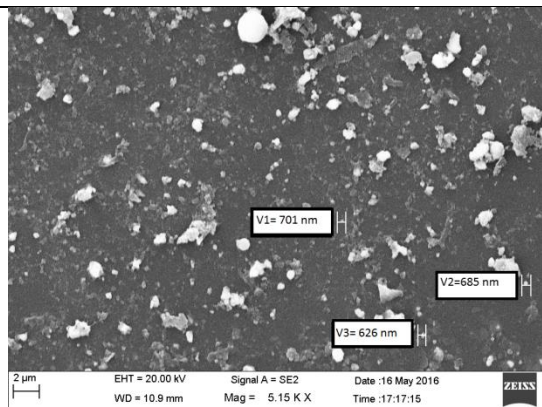


**Observation:** Particles are irregular in shape. Agglomerated and mono dispersed particles are found at different places.

**Conclusion:** Due to very high concentration and time

---

6      7.5      10      30      550

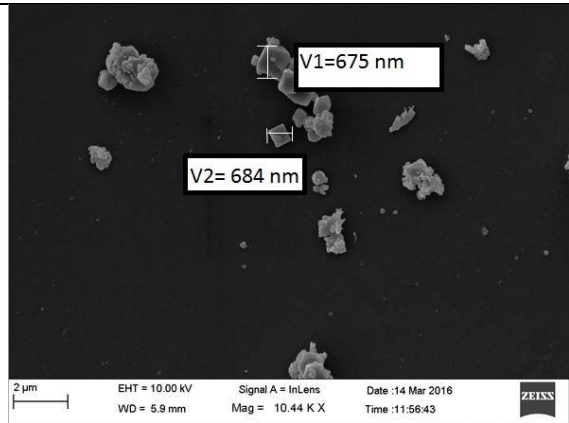


**Observation:** Particles are irregular in shape. Agglomerated particles are formed

**Conclusion:** Due to high concentration

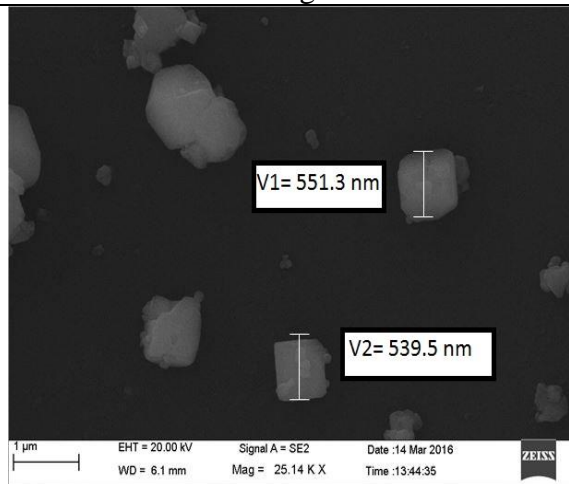
---

7 10 5 30 665



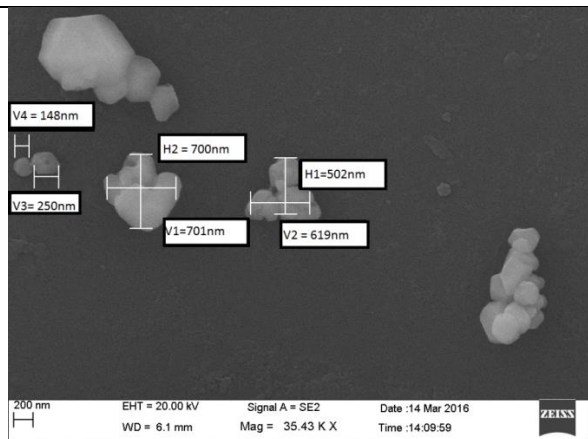
**Observation:** Particles are irregular in shape.  
Agglomerated particles are formed  
**Conclusion:** Due to high concentration

8 7.5 5 15 535



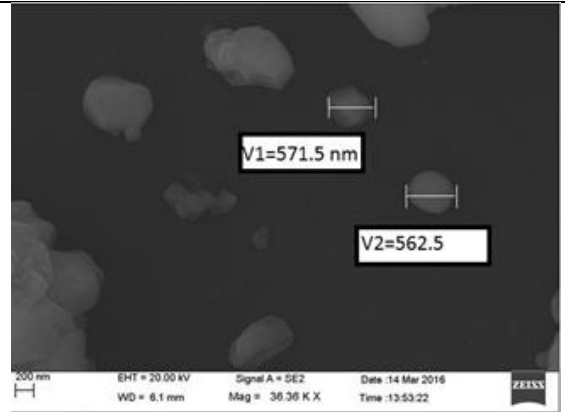
**Observation:** Particles are agglomerated and rectangular at some places  
**Conclusion:** Due to high concentration IEG and less time

9 5 10 45 180



**Observation:** Particles are agglomerated and rectangular at some places  
**Conclusion:** Due to high operating time

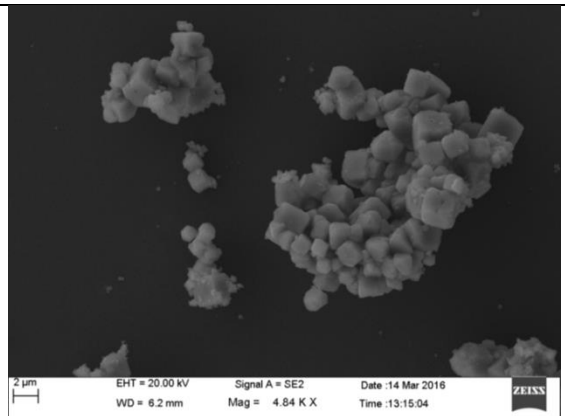
10      7.5      5      45      560



**Observation:** Agglomeration of particles is reduced.

**Conclusion:** Due to reduction in electrolytic concentration

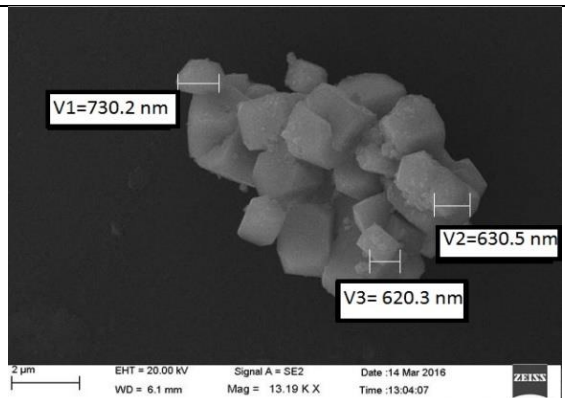
11      7.5      15      45      570



**Observation:** Agglomerated particles is formed

**Conclusion:** Due to high concentration and time

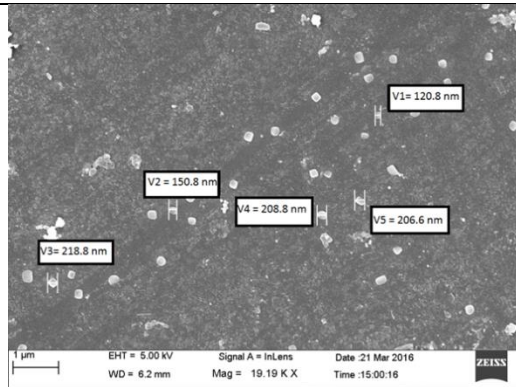
12      10      10      30      650



**Observation:** Cluster of particles is formed

**Conclusion:** Due to high electrolytic concentration and IEG

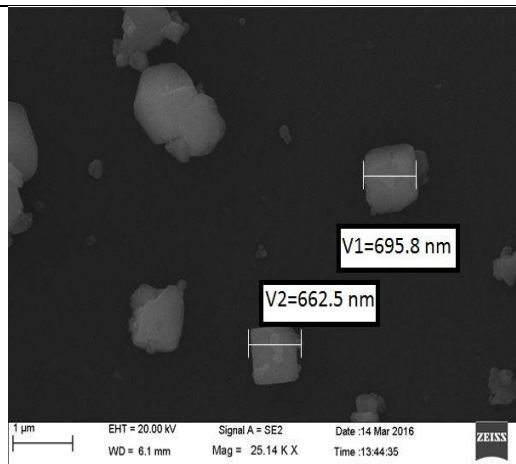
13      5      10      30      150



**Observation:** Uniform size rectangular particles is obtained

**Conclusion:** Due to less electrolyte concentration

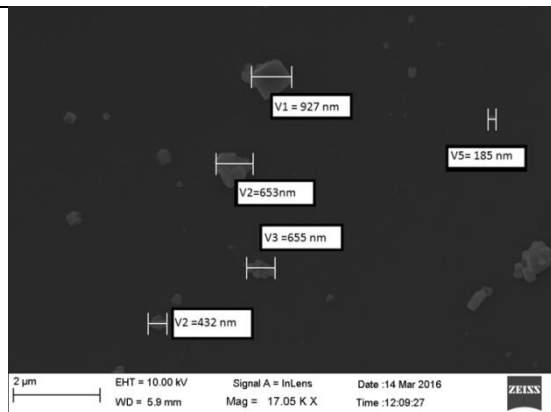
14      10      15      30      670



**Observation:** Larger particles size is observed

**Conclusion:** Due to high electrolytic concentration and IEG

15      7.5      10      45      555



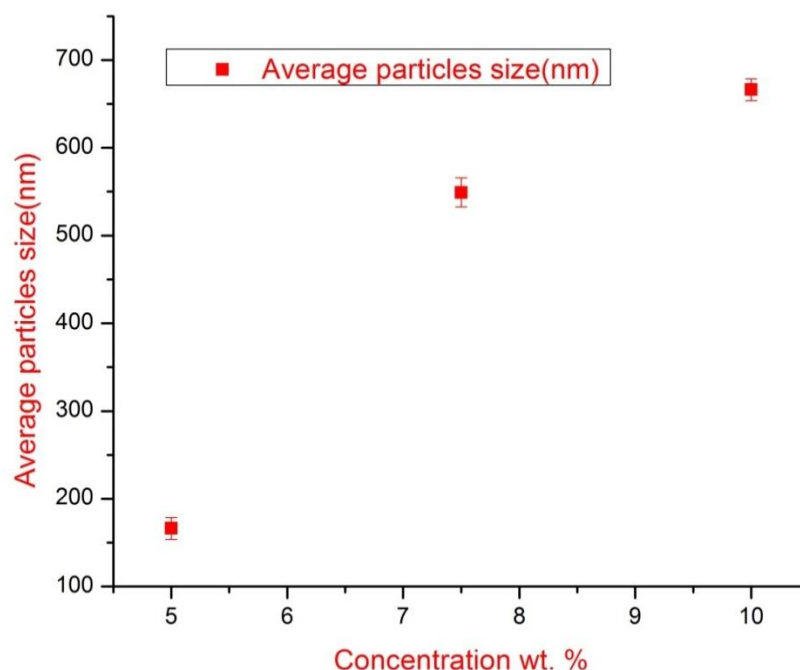
**Observation:** Larger particles size is observed

**Conclusion:** Due to high electrolytic concentration and time

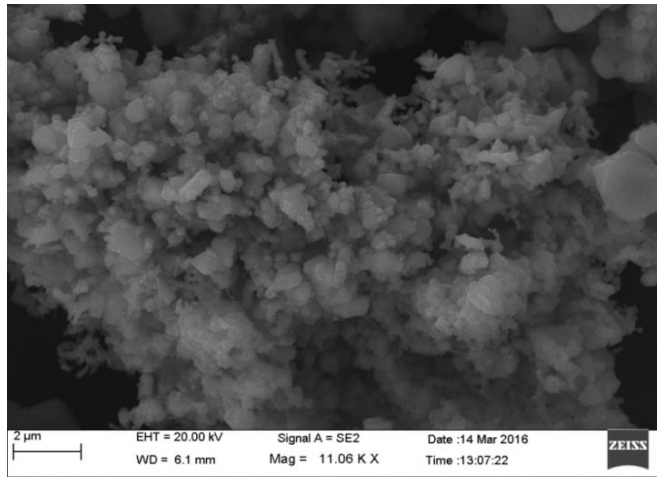
### 5.1.1 Effect of Electrolyte Concentration

Figure 5.1 graphically depicts the effect of electrolyte concentration on the average size of copper nano-particles, showing that an increase in electrolyte concentration results in larger nano-particles of copper. This is due to increased agglomeration of copper nano-particles with an increase in electrolyte concentration, which causes more particles to interact with the cathode plate. As shown in Fig. 5.1, as electrolyte concentration increases from 5% to 10%, the average size of nano-particles increases from 150 to 600 nm. Figure 5.2 shows SEM images which depict the effect of electrolyte concentration on the size of copper nano-particles. The size of the copper nano-particles decreases due to reduced agglomeration when the concentration of the electrolyte is decreased to 7.5% (Fig. 5.2b) and 5% (Fig. 5.2c) from 10% (Fig. 5.2a), at which clusters of nano-particles are formed.

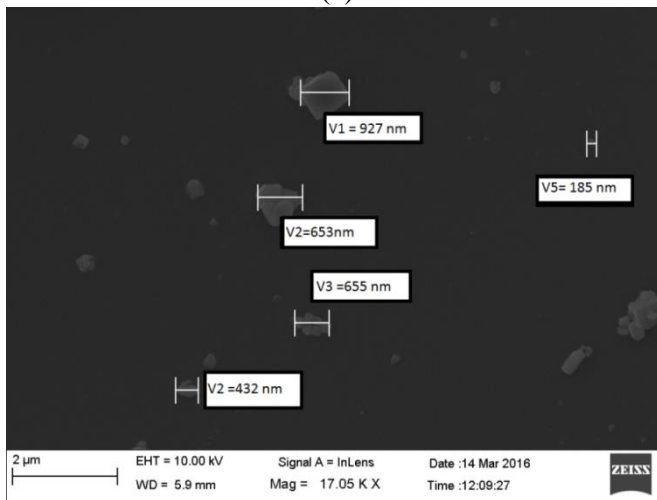
When the concentration of the electrolyte was increased up to 50% and electrolytic action was allowed for more than 1 hour, a very thin layer having 0.3 mm thickness of electroplated copper was obtained on the cathode plate as shown in Fig. 5.3. This is due to the fact that higher concentration causes a larger number of particles to move from anode to cathode. Coating is obtained when these particles get ample time to adhere onto the cathode plate.



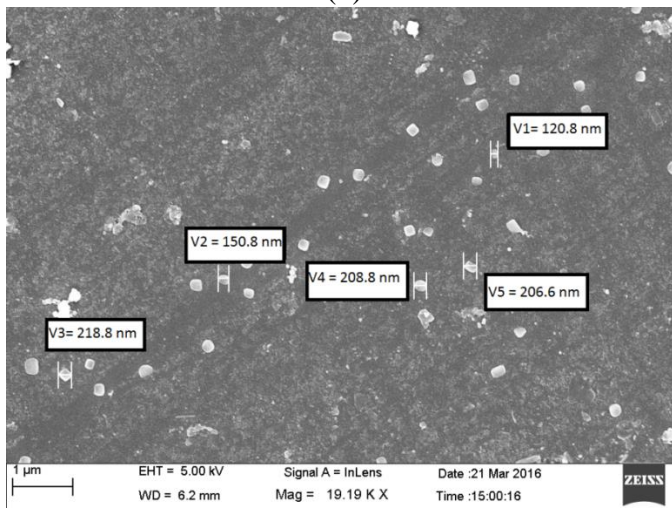
**Fig. 5.1:** Effect of electrolyte concentration on average size of copper nano-particles.



(a)



(b)



(c)

**Fig. 5.2:** SEM images of the copper nano-particles generated in 45 minutes using IEG as 10 mm (a) agglomerated nano-particles using electrolyte concentration as 10%; nano-particles with reduced agglomeration using electrolyte concentration (b) 7.5%; and (c) 5%.

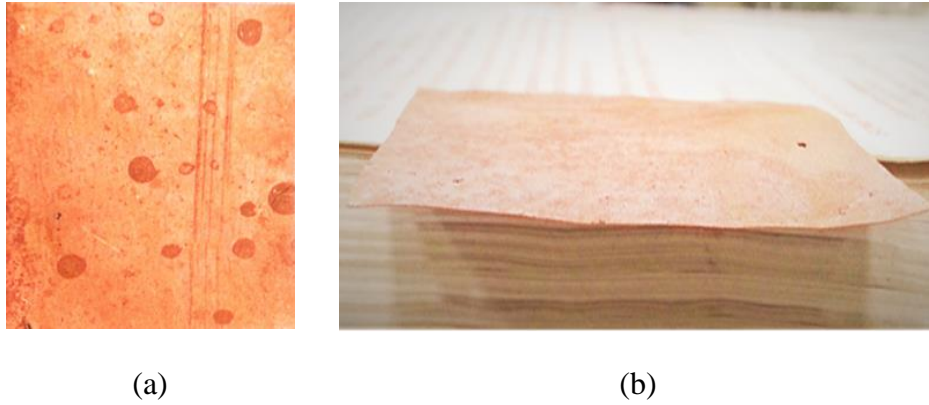


**Fig. 5.3:** Photographs of the thin layer of copper coated on the cathode plate in 1 hr by PECD process using 50% electrolyte concentration (front view); (b) side view showing thickness of thin film of copper.

### 5.1.2 Effect of Inter-electrode Gap

Figure 5.4 shows variation in average size of copper nano-particle size with IEG. It can be seen from this Figure smaller IEG (5 mm) results in larger nano-particles this is due to the fact that current density is inversely proportional to IEG which means at lesser the IEG, current density will be higher which results in higher material removal rate (MRR) leading more number of copper particles moving towards cathode plate causing agglomeration of particles thereby in larger size of nano-particles. When IEG is high (15 mm) then less number of particles will reach to the cathode plate and less number of nano-particles will be formed SEM images 5.5(a), 5.5(b), 5.5(c) shows the nano-particles at different inter electrode gap. SEM image 5.4(a) shows clusters of particles formed at IEG of 5 mm, agglomeration of particles is reduced when IEG is increased to 10 mm which is depicted in SEM image 5.5(b). Size of the particles is increased when IEG is increased to 15 mm.

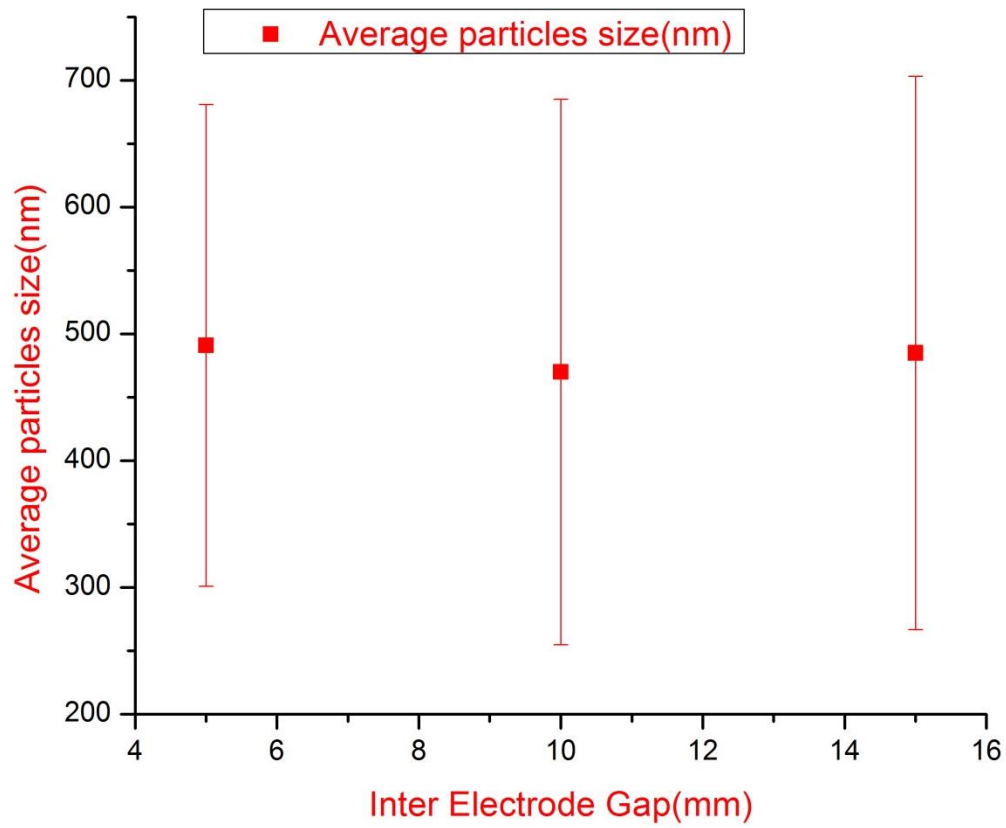
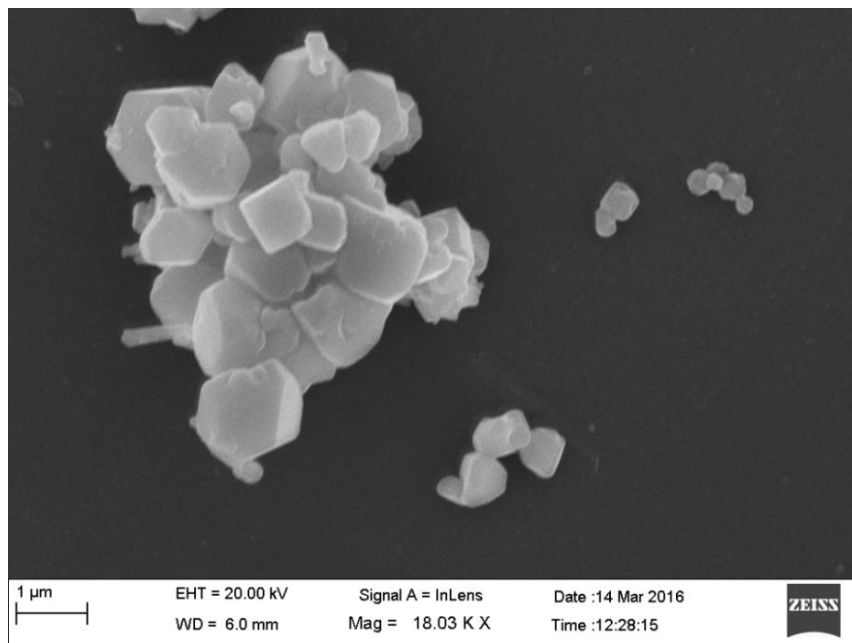
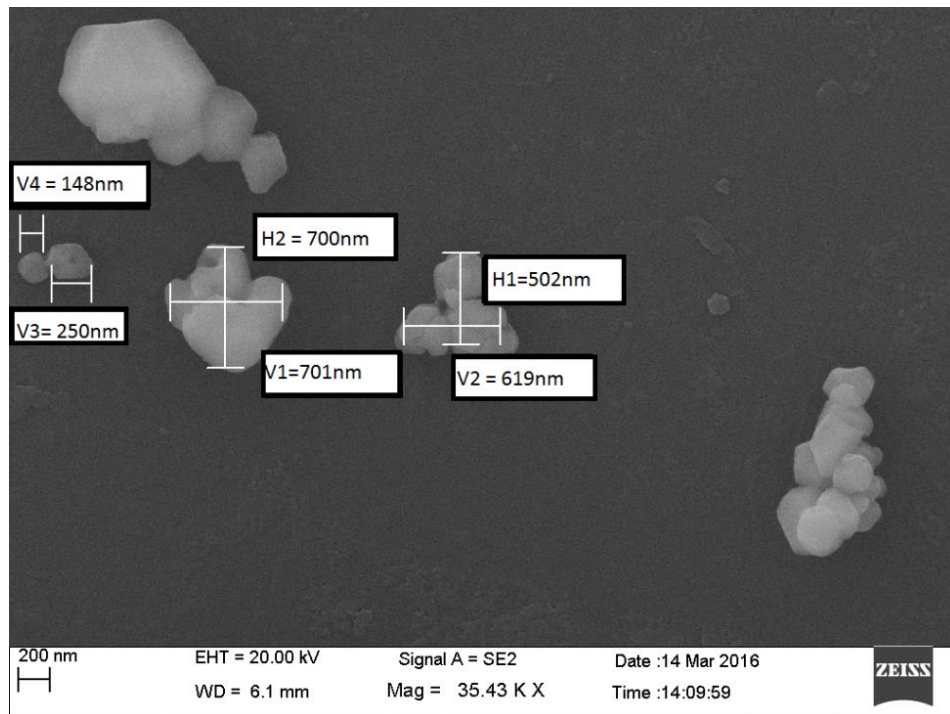


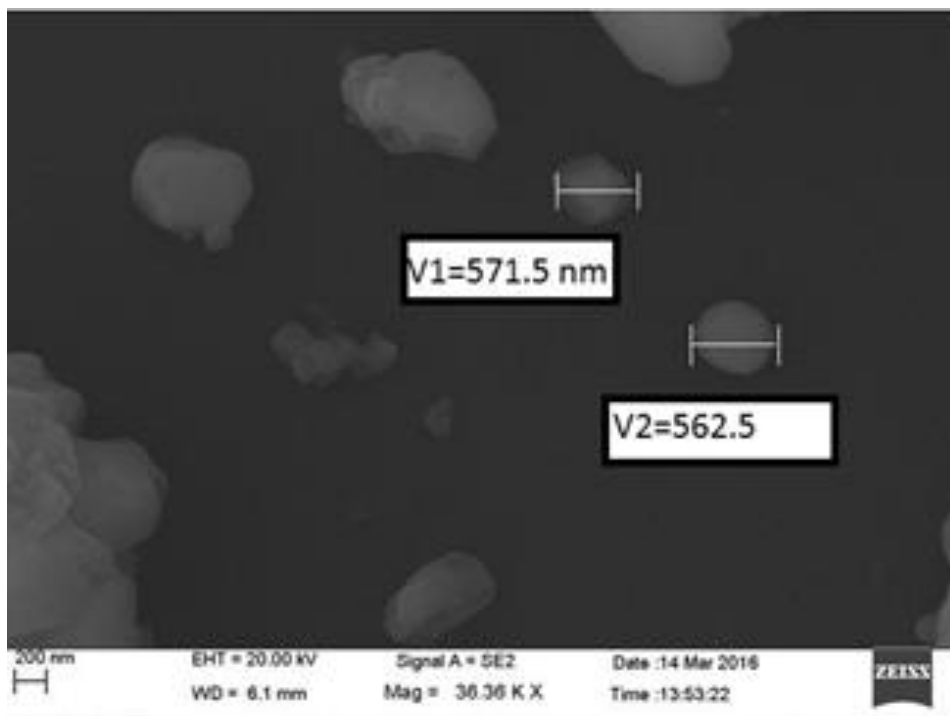
**Fig. 5.4:** Effect of inter-electrode gap on average size of copper nano-particles.



(a)



(b)



(c)

**Fig 5.5:** SEM images of the copper nano-particles generated in electrolyte concentration 7.5 wt.% using time as 15minutes (a) agglomerated nano-particles using IEG as 5 mm; nano-particles with reduced agglomeration using electrolyte concentration (b) 10mm; and (c) 15 mm.

### 5.1.3 Effect of Time

Electrolysis time is one of the major concerns in electrochemical synthesis, since longer times may lead to higher energy consumption. In the current study, increases in reaction time generally resulted in increased corrosion of the anode which produced more  $\text{Cu}^{+2}$  ions in the aqueous phase solution. Effect of time on nano-particles size is shown in fig 5.6. It shows the nano-particles size in three time level .Nano-particle size at 15 minutes is 475 nm, at 30 minutes is 350 and 480nm when time is 45 minutes. Size of the particles have been decreasing when time is increased from 15 to 30 minutes and again decreasing when time is increased from 30 to 45 minutes time so there should be sufficient time for the formation of nano-particles at the cathode plate. When time is 15 minutes, very thin layer of copper is formed. It takes more than 15 minutes to form nano-particles at the cathode plate, if the process is given more time (>30 minutes) then agglomeration of particles is formed which results in larger particles size of the particles. SEM images 5.7(a) and 5.7(b) shows the variation of nano-particles size along with time.

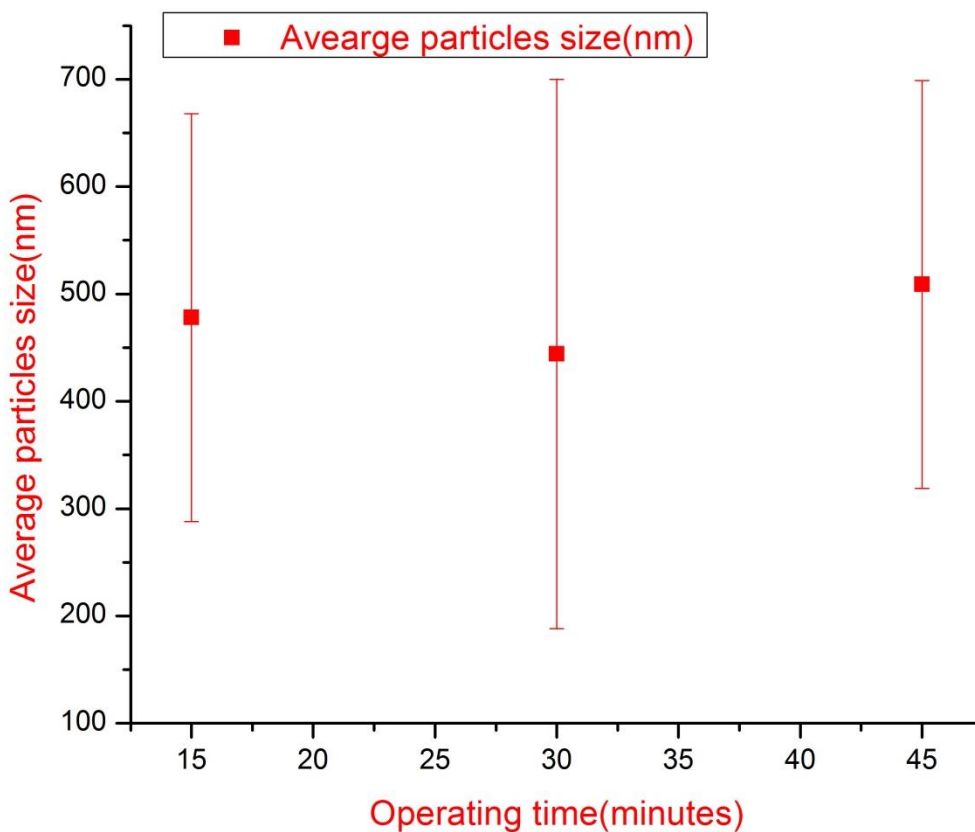
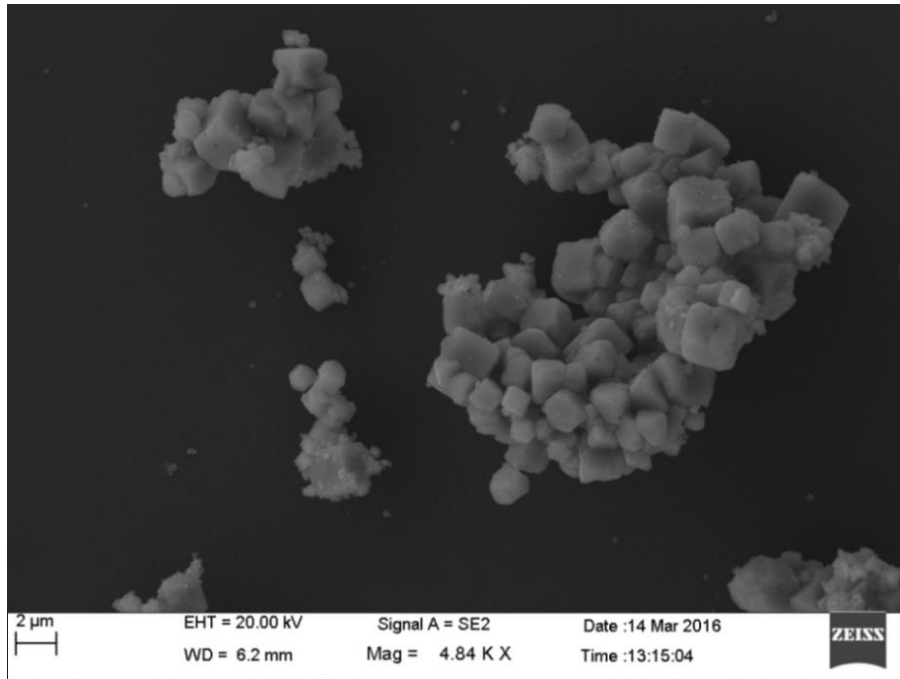
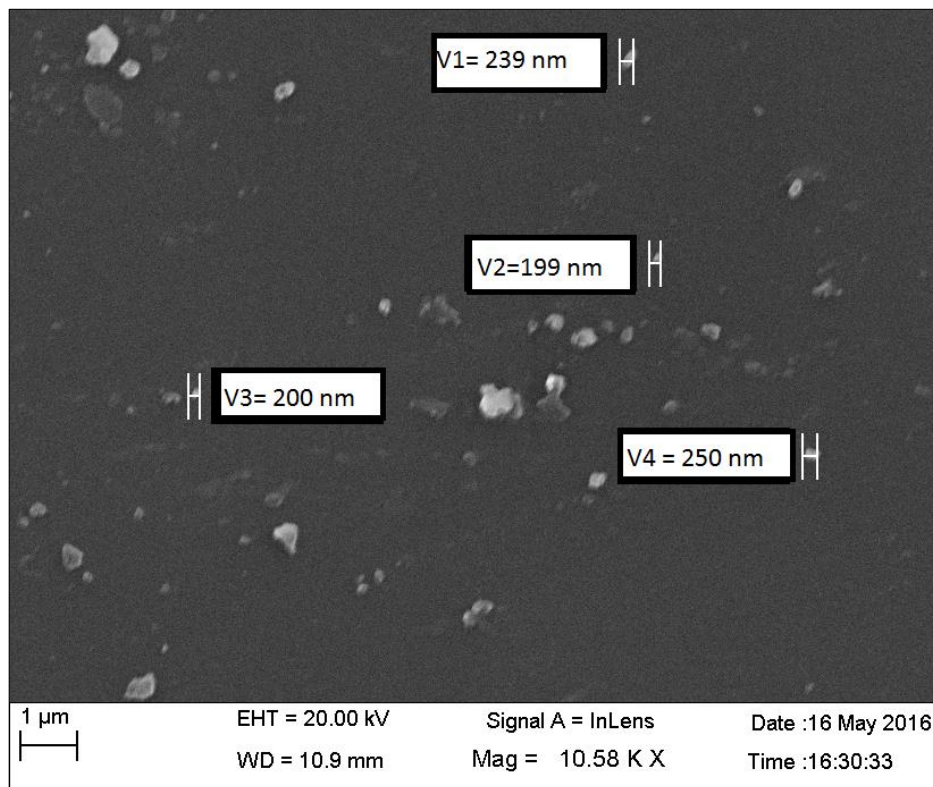


**Fig 5.6:** Effect of operating time on average size of copper nano-particles.



(a)



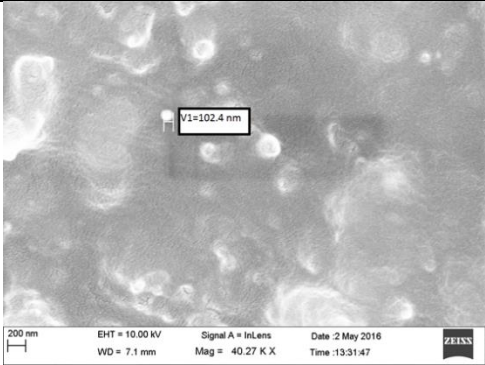
(b)

**Fig 5.7:** SEM images of the copper nano-particles generated in electrolyte concentration 10 wt.% using IEG as 10mm (a) agglomerated nano-particles using operating time as 45 minutes; nano-particles with reduced size of the particles using operating time (b) 30 minutes.

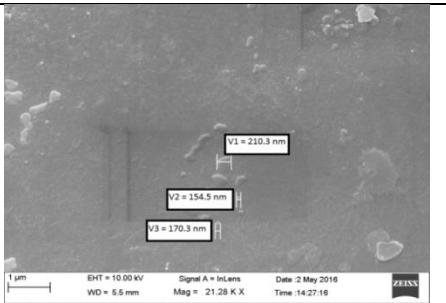
## 5.2 Main experiments

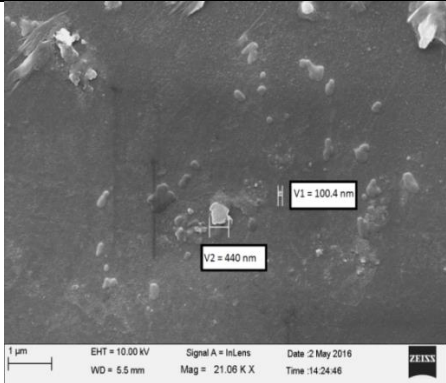
Main experiments were performed to obtain optimum size of the nano-particles. Based on the results of the pilot experiments, optimum value of three parameters were determined for the main experiments to obtain best morphology of the nano-particles. The main experiments were designed using response surface methodology (central composite design). In these experiments, nano-particles morphology and chemical composition were investigated. Table 5.2 list the size of the nano-particle obtained in the main experiments.

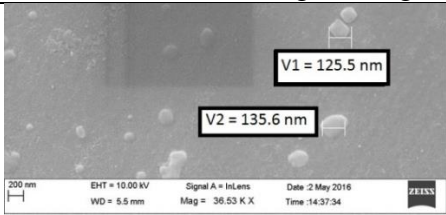
**Table 5.2:** Average size of the generated copper nano-particles and their SEM images for different input parameters combinations in 27 main experiments.

| Exp. No. | Voltage 'V' (volts) | Pulse-on time ' $T_{on}$ ' (ms) | Pulse-off time ' $T_{off}$ ' (ms) | Size of copper nano-particles (nm)   | SEM image, observations and conclusions  |
|----------|---------------------|---------------------------------|-----------------------------------|--------------------------------------|--|
| 1        | 8                   | 2                               | 8                                 | Nano-particles could not be obtained |  |
| 2        | 12                  | 4                               | 8                                 | 102                                  |  <p><b>Observation:</b> Reduced particles size<br/> <b>Conclusion:</b> Due to optimized values obtained in pilot experiments</p>    |
| 3        | 12                  | 6                               | 8                                 | Nano-particles could not be obtained |  |
| 4        | 16                  | 2                               | 8                                 | 210                                  |  <p><b>Observation:</b> particles are segregated<br/> <b>Conclusion:</b> Due to optimized values obtained in pilot experiments</p> |

|   |    |   |    |                                      |
|---|----|---|----|--------------------------------------|
| 5 | 12 | 2 | 8  | Nano-particles could not be obtained |
| 6 | 12 | 2 | 12 | Nano-particles could not be obtained |
| 7 | 8  | 2 | 12 | Nano-particles could not be obtained |
| 8 | 8  | 2 | 4  | Nano-particles could not be obtained |

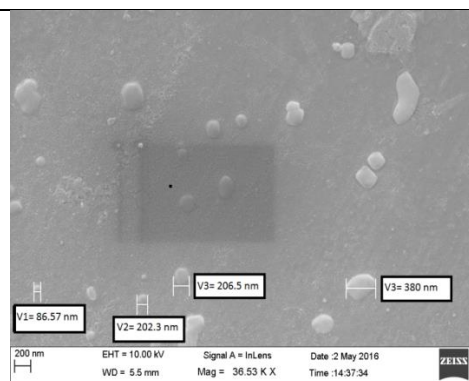
|   |    |   |    |     |   |
|---|----|---|----|-----|---|
| 9 | 16 | 4 | 12 | 211 |  <p><b>Observation:</b> Particles size is increased<br/> <b>Conclusion:</b> Due to high voltage</p> |
|---|----|---|----|-----|---|

|    |    |   |   |     |  |
|----|----|---|---|-----|--|
| 10 | 16 | 6 | 4 | 270 |  <p><b>Observation:</b> Particles size is increased<br/> <b>Conclusion:</b> Due to high voltage</p> |
|----|----|---|---|-----|--|

|    |   |   |   |     |   |
|----|---|---|---|-----|---|
| 11 | 8 | 6 | 4 | 130 |  <p><b>Observation:</b> Reduction in particles size<br/> <b>Conclusion:</b> Due to lower voltage</p> |
|----|---|---|---|-----|---|

---

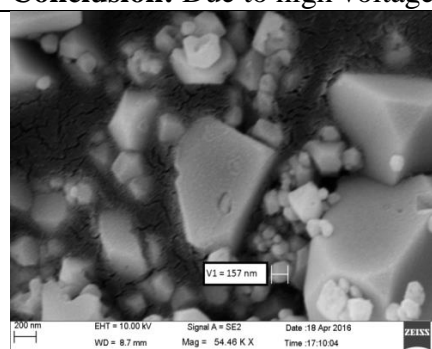
12      12      6      4      185



**Observation:** Mono disperse particles are formed  
**Conclusion:** Due to high voltage

---

13      12      2      4      157



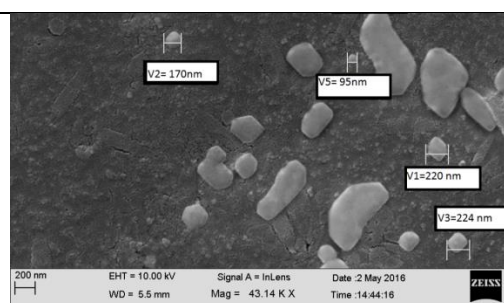
**Observation:** Agglomerated particles are formed  
**Conclusion:** Due to high voltage and less pulse-off time

---

14      16      2      4      Nano-particles could not be obtained

---

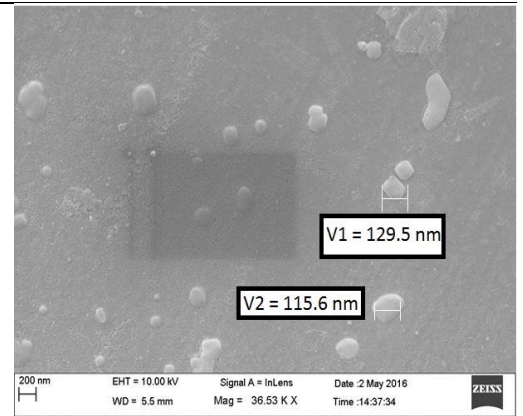
15      8      4      8      70



**Observation:** optimum size of nano-particles is obtained  
**Conclusion:** Due to optimum parameter obtained in main experiments

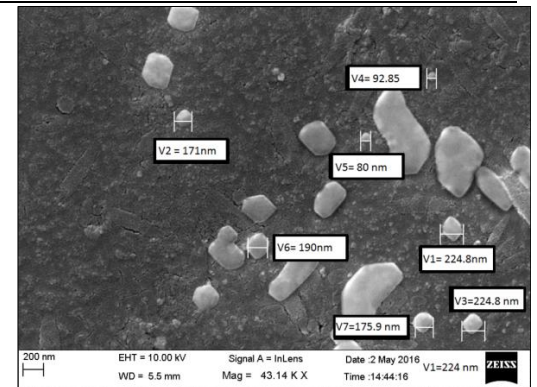
---

16 8 6 12 119



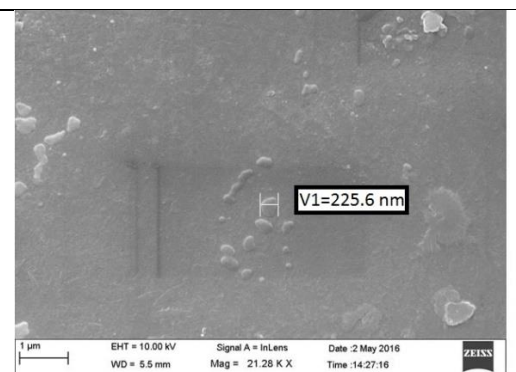
**Observation:** Agglomeration of particles is reduced  
**Conclusion:** Due to optimum value of voltage

17 8 4 12 85



**Observation:** Agglomeration of particles is reduced  
**Conclusion:** Due to optimum value of voltage and pulse-on time

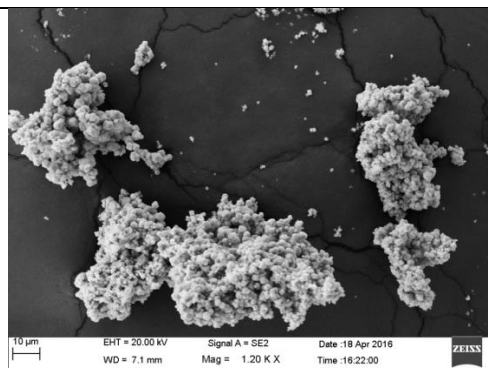
18 16 4 8 217



**Observation:** Increase in particles size  
**Conclusion:** Due to high voltage

---

19      16      4      4      225



**Observation:** Agglomerated particles are formed

**Conclusion:** Due to high voltage

---

20      16      6      8      Nano-particles could not be obtained

---

21      8      6      8      276

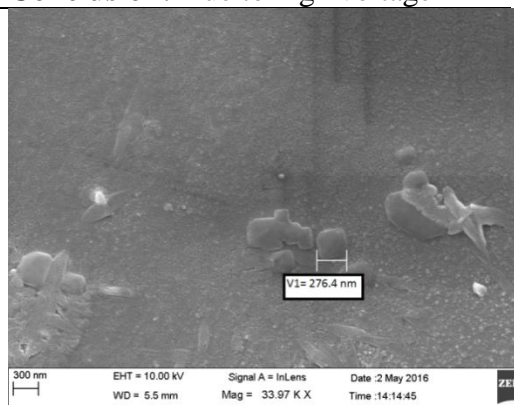


**Observation:** Particles size is increased

**Conclusion:** Due to high voltage

---

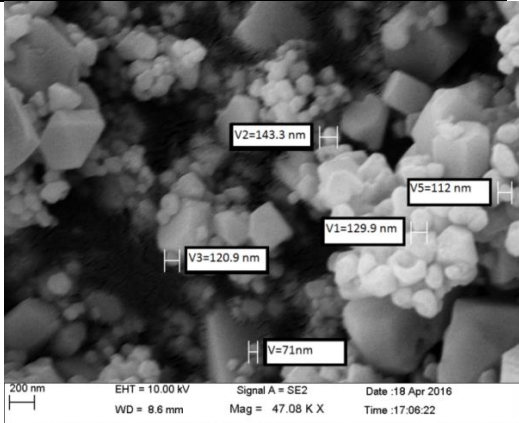
22      16      2      12      245



**Observation:** Number of particles formed is reduced

**Conclusion:** Due to less pulse-on time

---

|    |    |   |    |                                      |   |
|----|----|---|----|--------------------------------------|---|
| 23 | 16 | 6 | 12 | 271                                  |  <p><b>Observation:</b> Particles size is increased<br/><b>Conclusion:</b> Due to high voltage</p> |
| 24 | 12 | 4 | 4  | Nano-particles could not be obtained |   |
| 25 | 8  | 4 | 4  | Nano-particles could not be obtained |   |
| 26 | 12 | 4 | 12 | Nano-particles could not be obtained |   |
| 27 | 12 | 6 | 12 | Nano-particles could not be obtained |   |

### 5.2.1 Effect of Voltage

Voltage is one of major concerning parameter which should be optimized meticulously because it affects the electrochemical reaction in many ways. High cell voltages should not be used during electrochemical synthesis to avoid losses of energy, high temperatures, and electrode damage. Selection of the correct supporting electrolyte at an appropriate concentration can avail in minimizing the applied voltage for the electrochemical synthesis process. In the current study, increases in the applied voltage were observed to increase the corrosion percentage of the Cu anode that means nano-particle formation will increase. Higher applied voltage will results in following drawbacks

- ❖ Higher applied voltage will increase the temperature of the electrolyte which can damage the electrodes and it adversely affects the electrochemical reactions occurring inside the electrochemical cell.
- ❖ Rate of nucleation is increased by the application of higher overvoltage. Rate of nucleation (  $v$  ) can be expressed mathematically as shown in equation (Nekouei et al. 2013).

$$v = k_1 \exp\left(\frac{-k_2}{|\eta|}\right) \dots \dots \dots (1)$$

- ❖ Where  $K_1$  and  $K_2$  are constants; and  $\eta$  is the applied overvoltage. It is shown by the equation that application of higher over voltages increases the rate of nucleation rate ( $v$ ). The equation presented for very high over voltages is not correct, because in very high applied voltage, occurrence of auxiliary reactions (such as hydrogen evolution) leads to severe occurrence of polarization around the cathode. Also, since the hydrodynamic conditions adjacent to electrodes change, this equation cannot be used in very high current density in direct current state. The critical overvoltage for this equation depends on different factors such as type of current and the additives.
- ❖ Application of higher voltage ( $> 15V$ ) may reduce the total reaction time but also increase the potential to form certain by-products such as Cu(II) oxides. Therefore, it was concluded that 8 V was the ideal applied voltage for the synthesis of Cu (II) to prevent the formation of undesired compounds.

As shown in equation 2 current density is directly proportional to voltage, if voltage is increased then current density will increase at the same rate which results in increased anodic dissolution. Due to increased anodic dissolution, particles depositing on the cathode will be increased and chances of agglomeration of particles will be increased. Variation of nano-particles size along with voltage is shown in fig 5.8. At higher voltage more number of copper particles is depositing on the cathode resulting in agglomeration of nano-particles which is shown in fig 5.9(a). Lower voltage results in small size of nano-particles which is shown in fig 5.9(b).

$$J = \text{Current density (A/mm}^2\text{)} = \frac{I}{A_p} = \frac{1}{A_p} \frac{V - \Delta V}{R} \dots \dots \dots .2$$

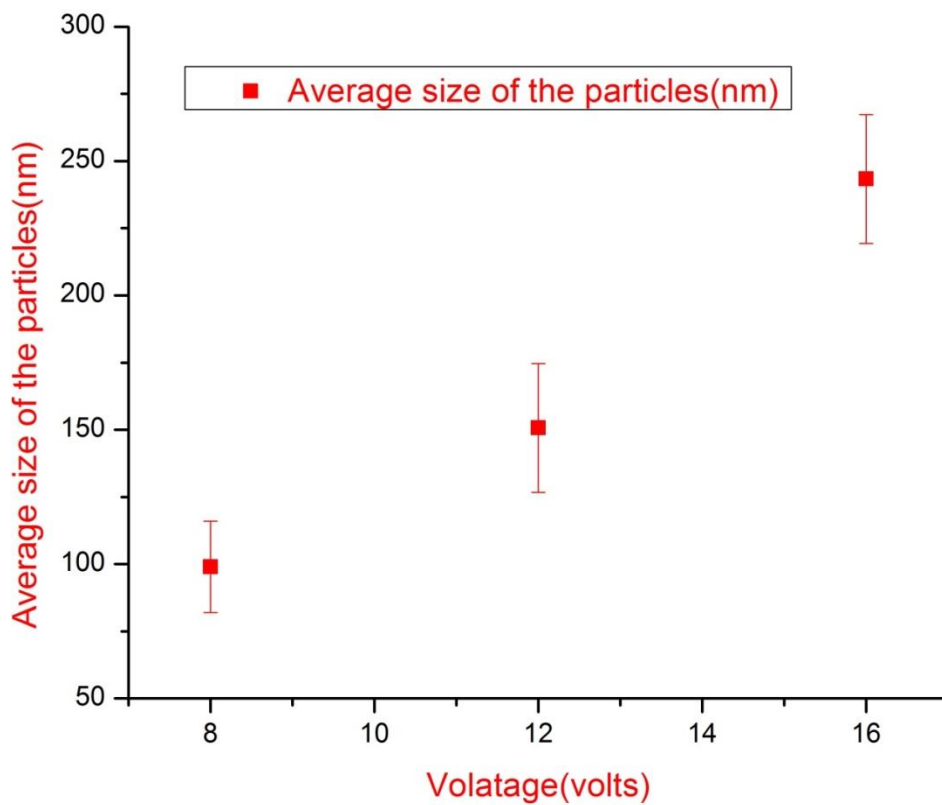
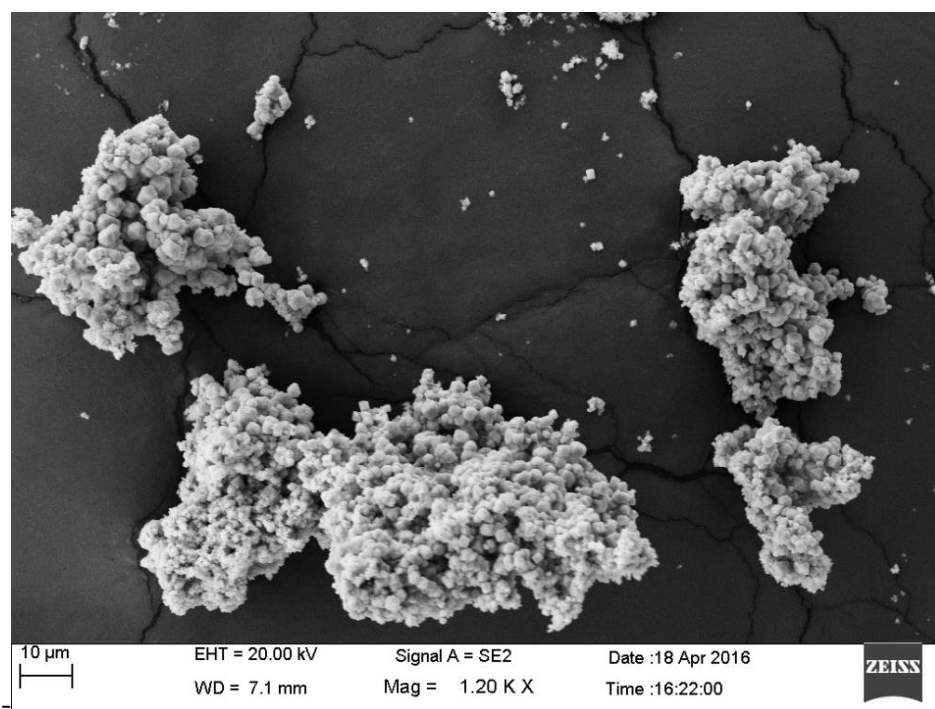
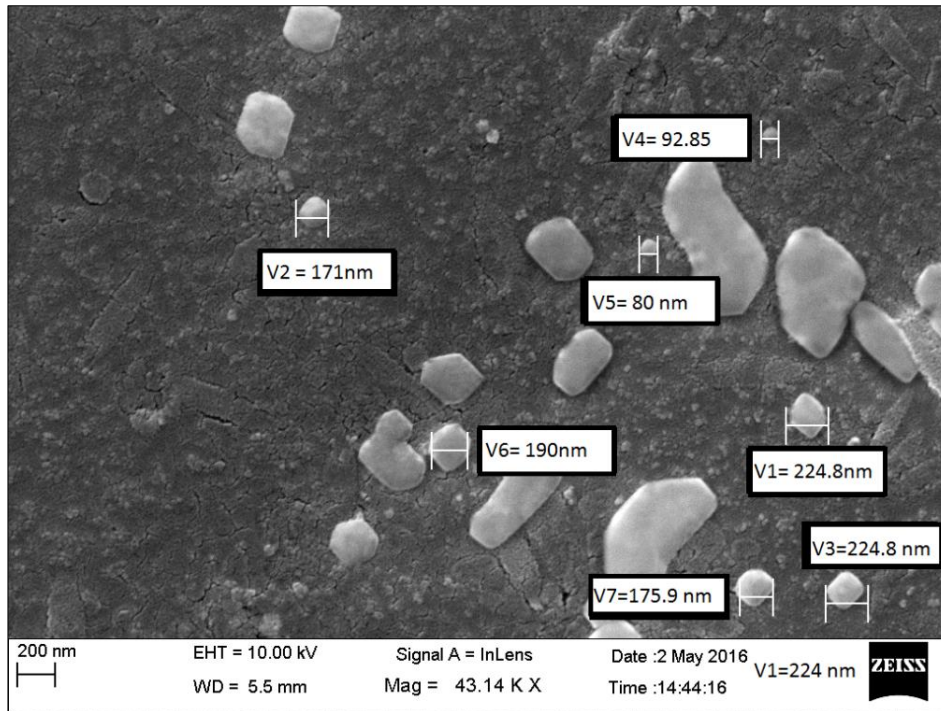


**Fig 5.8:** Effect of voltage on average size of copper nano-particles



(a)

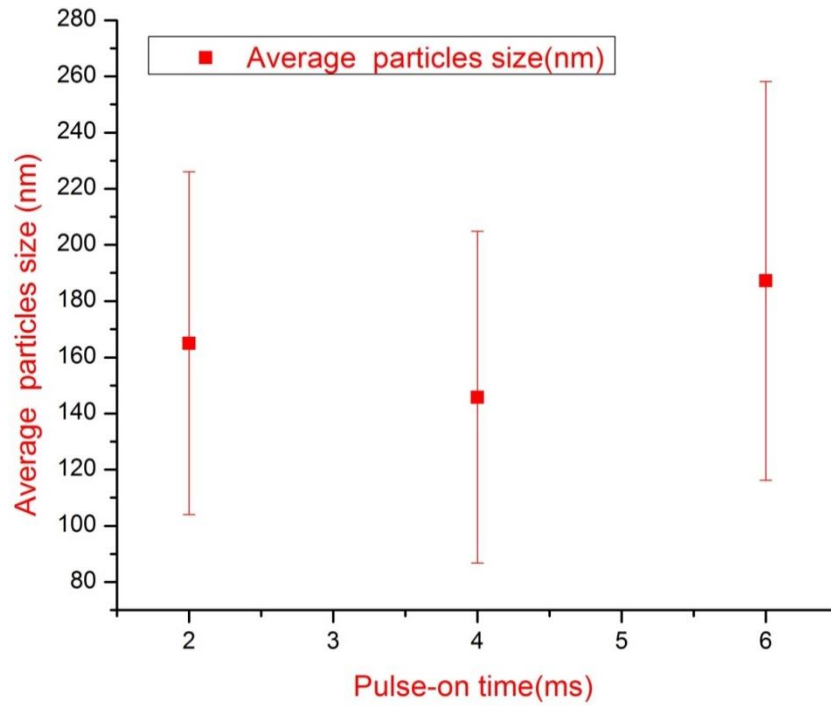


(b)

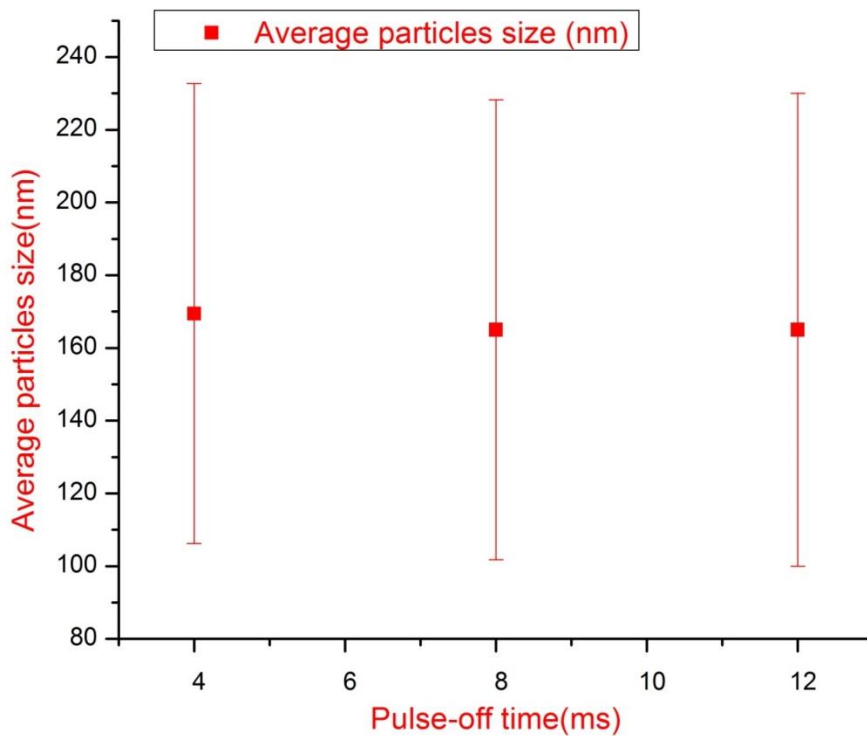
**Fig 5.9:** SEM images of the copper nano-particles generated in pulse-on time 6 ms using pulse-off time as 4 ms (a) agglomerated nano-particles using voltage as 16V; nano-particles with reduced size of the particles using voltage (b) 8V

### 5.2.2 Effect of Pulse-on Time and Pulse-off time

Lower pulse-on time restricts current to generate less number of nano-particles and operating time is not sufficient for generation of large amount of nano-particles. On the other hand higher value of Pulse-on time will lead to more anodic dissolution of the anodic plate and generating large number of nano-particles. In both cases large size of nano-particles is obtained. This is confirmed with the optimum value of pulse-on time being obtained as 4ms. Pulse off time does not affect the size and the shape of the nano-particles. Experimental results confirm that variation of pulse-off time does not affect nano-particles size. Fig 5.10 (a) shows the variation of average particles size along with pulse-on time. It is evident from the figure that nano-particles size is minimum at pulse-on time of 4 ms. Figure 5.10(b) illustrates the variation of average particles size along with pulse-off time. It is confirmed from the figure that average particles size is not so much affected by pulse-off time. Fig 5.11(a) and 5.11(b) shows the SEM image of particles obtained 6 ms and 4 ms. It is evident from figures that size of the particles reduces when pulse-on time decreases.

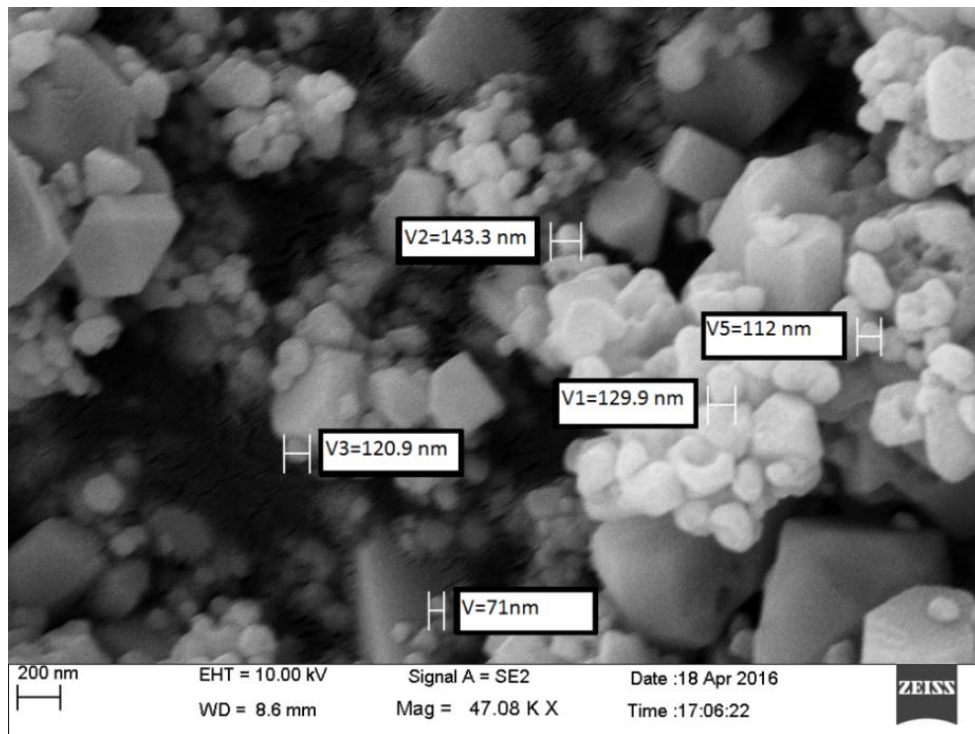


(a)

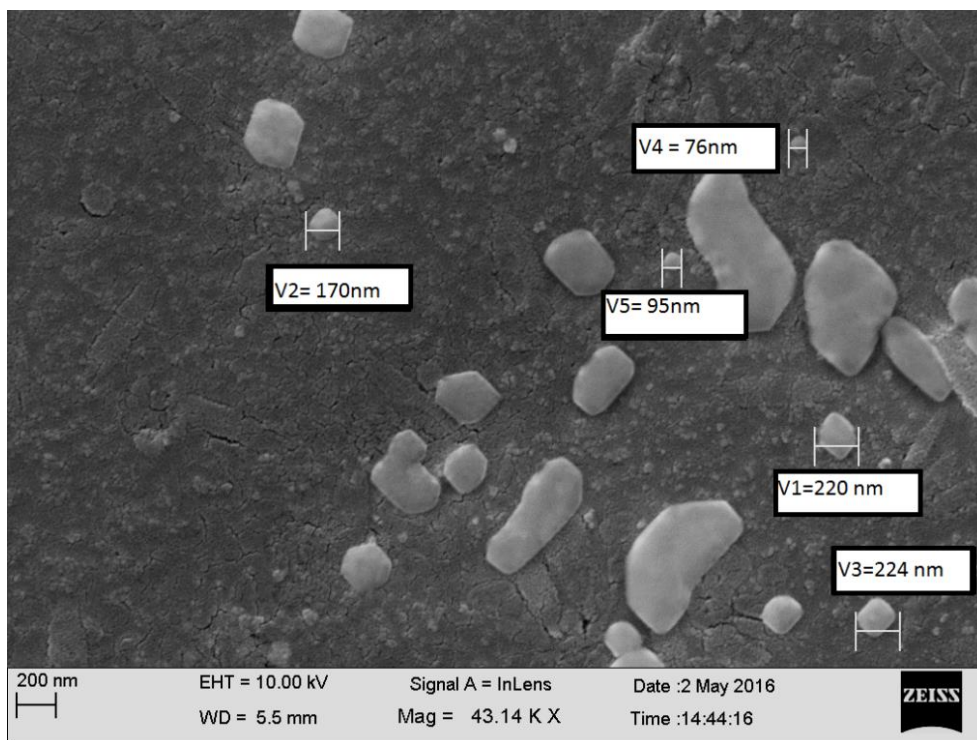


(b)

**Fig 5.10:** (a) Effect of pulse-on time on average size of copper nano-particles (b) Effect of pulse-off time on average size of copper nano-particles.



(a)



(b)

**Fig 5.11:** SEM images of the copper nano-particles generated in Voltage 8V using pulse-off time as 8 ms (a) agglomerated nano-particles using pulse-on time as 6 ms; nano-particles with reduced size of the particles using pulse-on time (b) 4ms

### 5.3 Analysis of Chemical Composition and Morphology

This section focuses on the elemental distribution and crystal structure of the particles obtained by the electro chemical dissolution. XRD and EDX analysis shows the elemental distribution and crystal structure of the particles obtained by the process. Theivasanthi and Alagar (2010) studied X Ray Diffraction of Copper Nano-particles. Three peaks at  $2\theta$  values of 43.640, 50.800, and 74.420 deg corresponding to (111), (200), and (220) planes of copper were observed. In the present work, it was observed that generated copper particles peaks found at  $2\theta$  values of 44, 51, and 74 degrees corresponding to (111), (200), and (220) planes of copper. It shows that generated copper particles are pure. Peaks obtained are sharp which show copper particles are highly crystalline. Crystal structure of generated copper particles is face centered cubic and following calculations can be used to determine the crystal structure of the particles as shown below.

- ❖ Standard unit cell length of FCC copper  $a = 3.60 \text{ \AA}$
- ❖ Wavelength  $\lambda = 1.5418 \text{ \AA}$  for Cu Ka
- ❖ Bragg's Law:  $2d\sin\theta = n \lambda$  .....(3)

Formula used in the calculation of the *expected  $2\theta$  positions of the first three peaks* in the diffraction pattern and the *interplanar spacing  $d$*  for each peak.

- ❖  $1/d^2 = (h^2+k^2+l^2) / a^2$  ..... (4)

Bragg's Law is used to determine the  $2\theta$  value:  $\lambda = 2d_{hkl} \sin \theta_{hkl}$

**1) hkl = 111**

$$1/d^2 = (1^2 + 1^2 + 1^2) / (3.60 \text{ \AA})^2 \rightarrow d = 2.078 \text{ \AA}$$

$$\sin\theta_{111} = 1.54 \text{ \AA} / \{2(2.078 \text{ \AA})\} \rightarrow \theta = 21.75^\circ (2\theta = 43.5^\circ)$$

**2) hkl = 200**

$$1/d^2 = (2^2 + 0^2 + 0^2) / (3.60 \text{ \AA})^2 \rightarrow d = 1.8 \text{ \AA}$$

$$\sin\theta_{200} = 1.54 \text{ \AA} / \{2(1.8 \text{ \AA})\} \rightarrow \theta = 25.3^\circ (2\theta = 50.6^\circ)$$

**3) hkl = 220**

$$1/d^2 = (2^2 + 2^2 + 0^2) / (3.60 \text{ \AA})^2 \rightarrow d = 1.274 \text{ \AA}$$

$$\sin\theta_{220} = 1.54 \text{ \AA} / \{2(1.274 \text{ \AA})\} \rightarrow \theta = 37.25^\circ (2\theta = 74.5^\circ)$$

These expected  $2\theta$  values are very close with the standard  $2\theta$  values mentioned by Theivasanthi and Alagar (2010). This is confirmed that obtained copper particles have FCC crystal structure. Fig 5.12 shows the *Miller Indices* (h k l) of three most intense peaks.

Energy Dispersive X-rays analysis is an analytical technique used for the chemical characterization of a sample to map out the lateral distribution of elements from the imaged

area Fig 5.13 shows elemental distribution of the material Results obtained by EDX shows that copper with very less amount of oxygen impurity is obtained through ECD process.

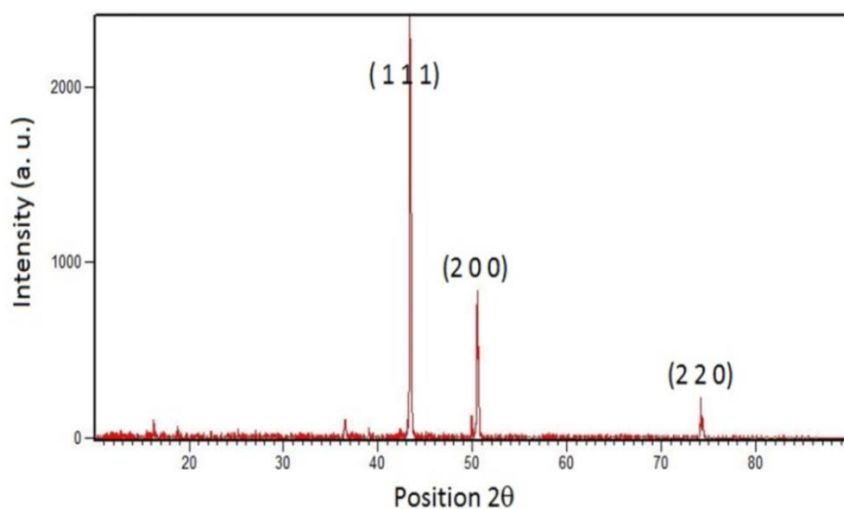


**Fig 5.12:** XRD analysis of copper nano-particles.

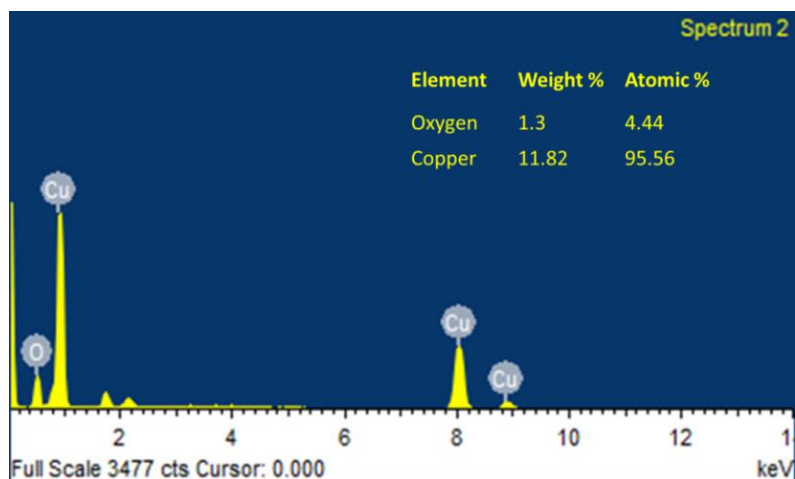


**Fig 5.13:** Elemental distribution of the material.

The *next chapter* highlights the conclusions derived from the present work and scope for future work based on the limitations of the present work.

## Chapter 6

### Conclusions and Scope for Future Work

This chapter summarizes the significant achievements and conclusions from the present work, highlighting the extent to which the aims and objectives are met. It also presents the possibilities for future work based on the outcomes of the research.

#### 6.1 Conclusions

Following conclusions can be made from present research work.

- Electrolytic concentration, operating time ( $t$ ), IEG, voltage (V) and Pulse-on time ( $T_{on}$ ) are found to be most important parameters in generating uniform size nanoparticles.
- Based on the results of the pilot experiments, optimum value of three parameters (electrolytic concentration 5wt. %, operating time: 30 minutes, IEG: 10mm) were determined for the main experiments.
- Under present experimental apparatus decrease in electrolytic concentration and voltage reduces the particle size.
- Present study shows that optimum value of operating time, IEG, Pulse-on time ( $T_{on}$ ) and Pulse-off time ( $T_{off}$ ) are found to be 30 minutes, 10mm, 4 ms and 8ms respectively.
- Very high concentration (50 wt. %) of electrolyte results in the formation of thin layer (.3mm) of copper on the cathode plate.
- The range of particles size is 70 nm to 800 nm obtained by ECD. Minimum average size of the copper particles is found to be 70 nm with a narrow size particles distribution and shape of the particles was irregular.
- It was observed that generated copper particles peaks found at  $2\theta$  values of 44, 51, and 74 degrees corresponding to (111), (200), and (220) planes of copper. It shows that generated Peaks obtained are sharp which indicates that copper particles are pure and highly crystalline
- EDX results shows that copper with very less amount of oxygen impurity is obtained through ECD process
- ECD process is ecologically safe, pollution free process, which is desirable for our environment protection.

**Table 6.1:** Process parameters and range of the particles obtained from main and pilot experiments.

| <b>S. NO</b>             | <b>Process parameter</b> | <b>Levels</b>                      | <b>Range of particles size</b> |
|--------------------------|--------------------------|------------------------------------|--------------------------------|
| <b>Pilot experiments</b> |                          |                                    |                                |
| 1                        | Concentration            | 5, 7.5 and 10 wt. % (3 levels)     | 150 to 700 nm                  |
| 2                        | IEG                      | 5, 10 and 15 mm (3 levels)         | 150 to 700 nm                  |
| 3                        | Operating Time           | 15, 30 and 45 min (3 levels)       | 150 to 700 nm                  |
| <b>Main experiments</b>  |                          |                                    |                                |
| 1                        | Voltage                  | 8, 12 and 16 V (3 levels)          | 70 to 250 nm                   |
| 2                        | Pulse-on time            | 2, 4 and 6 milliseconds (3 levels) | 70 to 250 nm                   |
| 3                        | Pulse-off time           | 4,8 and 12 milliseconds (3 levels) | 70 to 250 nm                   |

## 6.2 Scope for Future Work

1. Exploring use of ECD to generate nano-particles for other electrically conductive material i.e. aluminum, gold, titanium
2. Additive can be added in the electrolytic solution to reduce agglomeration of the particles.

## References

- Boutinguiza, M., Vala, J.D., Riveiro, A., Lusquiños, F., Quintero, F., Comesañac, F., Pou, J., 2013**, Synthesis of titanium oxide nano-particles by Ytterbium fiber laser ablation, *Physics Procedia* 41, 787 – 793.
- Chang, S., Teng, T., Ismail, N., 2011**. Screening of factors influencing Cu(II) extraction by soybean oil-based organic solvents using fractional factorial design, *Journal of Environmental Management*, 92, 2580–2585.
- Horikoshi, S., Serpone, N., 2013**. *Microwaves in Nanoparticle Synthesis*, First Edition.
- Khan, A., Rashid, A., Younas, R., Chong, R., 2016**. A chemical reduction approach to the synthesis of copper nano-particles, *Int Nano Lett* 6:21–26.
- Ma, H.K., Pan, T.J., Cheng, P.T., 2014**, Numerical Study of the Nanoparticle Formation Mechanism in a Titania Flame Combustion Synthesis Process, *Aerosol and Air Quality Research*, 14: 251–259.
- Maksimović, V., Pavlović Lj., Pavlović, M., Tomić, M., 2006**. Morphologies of copper deposits obtained by the electrodeposition at high over potentials, *Surface and Coating Technology*, 201, 560–566.
- Maksimović, V., Pavlović Lj., Pavlović, M., Tomić, M., 2009a**. Characterization of copper powder particles obtained by electro deposition as function of different current densities, *Journal of Applied Electrochemistry*, 39, 2545–2552.
- Maksimović, V., Pavlović Lj., Pavlović, M., Tomić, M., 2009b**. Characterization of copper powder particles obtained by electrodeposition, *Savez inženjera metalurgije Srbije*, 15 (1) 19-27.
- Mbonyiryivuze, A., Zongo1, S., Diallo1, A., Bertrand, S., Minani1, E., Yadav, L.L., Mwakikunga1, B., Dhlamini1, S.M., Maaza., 2015**, Titanium dioxide nano-particles biosynthesis for dye sensitized solar cells application: Review, *Physics and Materials Chemistry*, 3(1), 12-17.
- Nekouei, R.K., Rashchi, F., Ravanbakhsh, A., 2013a**. Copper nanopowder synthesis by electrolysis method in nitrate and sulfate solutions, *Powder Technology*, 250, 91–96.
- Nekouei, R.K., Rashchi, F., Ravanbakhsh, A., 2013b**. Effect of organic additives on synthesis of copper nano powders by pulsing electrolysis, *Powder Technology* 237, 554–561.

- Nekouei, R.K., Rashchi, F., Ravanbakhsh, A., 2013c.** Using design of experiments in synthesis of ultra-fine copper particles by electrolysis, *Powder Technology* 237, 165–171.
- Pavlovic, M. Pavlovic, Lj., Maksimovic, V., Nikolic, N., Popov, K., 2010.** Characterization and morphology of copper powder particles as a function of different electrolytic regimes, *International Journal of Electrochemistry Science*, 5, 1862–1878.
- Raja, M., 2008.** Production of copper nano-particles by electrochemical process, *Powder Metallurgy and Metal Ceramics*, 47 (7–8), 402–405.
- Rodríguez-Sánchez, L., Blanco, M.C., López-Quintela, M.A., 2000.** Electrochemical synthesis of silver nano-particles, *J. Phys. Chem. B*, 104, 41.
- Ruparelia, J.P., Chatterjee, A.K., Duttagupta, S.P., Mukherji, S., 2008.** Strain specificity in antimicrobial activity of silver and copper nano-particles, *Acta Biomaterialia*, 4(3): 707.
- Sahu, R.K., Somashekhar S. Hiremath, S.S., Manivannan, P.V., Singaperumal, M., 2014a.** An innovative approach for generation of aluminum nano-particles by micro electrical discharge machining, *Procedia Materials Science* 5, 1205 – 1213.
- Sahu, R.K., Somashekhar S. Hiremath, S.S., Manivannan, P.V., Singaperumal, M., 2014b.** Generation and characterization of copper nano-particles using micro-electrical discharge machining, *Materials and Manufacturing Processes*, 29, 477–486.
- Sarathi, R., Sindhu, T.K., Chakravarthy, S.R., Sharma, A., Nagesh, K.V., 2008.** Generation and characterization of nano tungsten particles formed by wire explosion process, *Journal of Alloys and Compounds*, 475, 658–663.
- Sengar, A., Soni, P.R., 2014.** Preparation and characterization of near nano copper powder by electrolytic route, *International Journal of Nonferrous Metallurgy*, 3, 35-41.
- Singh, S.C., Gopal, R., 2007.** Zinc nano-particles in solution by laser ablation technique, *Bull. Mater. Sci.* 30, 291.
- Tantavichet, N., Damronglerd, S., Chailapakul, O., 2009.** Influence of the interaction between chloride and thiourea on copper electrodeposition, *Electrochimica Acta* 55, 240–249.
- Tesakova, M., Parfenyuk, V., 2010,** Effect of the anode material on the composition and dimensional characteristics of the nano-sized copper-bearing powders produced by the electrochemical method, *Surface Engineering and Applied Electrochemistry* 46 (5), 11–16.

- Theivasanthi, T., Alagar, M., 2010.** X-ray diffraction studies of copper nanopowder, *Archives of Physics Research*, 1(2):112-117.
- Theivasanthi, T., Alagar, M., 2011.** Nano sized copper particles by electrolytic synthesis and characterizations, *International Journal of the Physical Sciences*, 6(15), 3662-3671.
- Theivasanthi, T., Alagar, M., 2012.** Electrolytic synthesis and characterizations of silver nanopowder, *Nano Biomed. Eng*, 4(2), 58-65.
- Walker, R., Duncan, S., 1984.** The morphology and properties of electrodeposited copper powder, *Surface Technology*, 23, 301–321.
- Wankhede, P., Sharma, P.K., Jha, A.K., 2013.** Synthesis of copper nano-particles through wire explosion route, *Int. Journal of Engineering Research and Applications*, 3(6), 1664-1669.
- Wei, H., Xue-chen, D., Lei, Z., 2009.** Characterization of ultrafine copper powder prepared by novel electrodeposition method, *Journal of Center South University Technology*, 16 708–712.
- Wu, S.P., Meng, S.Y., 2006.** Preparation of micron size copper powder with chemical reduction method. *Materials Letters*, 60 (20), 2438–2442.
- Rajeshkanna, S., Nirmalkumar, O., 2014.** Synthesis and Characterization of Cu nano-particle Using High Energy Ball Milling Route and Compare with Scherrer Equation, *International Journal of Scientific Engineering and Research (IJSER)*, 2(12), 2347-3878
- Yanık, B., Agustos, H., Koyun, A., 2013.** Synthesis and Characterization of Aluminium Nanoparticles by Electric Arc Technique, *Arab J Sci Eng*, 38:3587–3592



## Appendix-A: Details of the Instrument Used

### ❖ Powdered XRD (PXRD)



|                 |  |
|-----------------|--|
| Make            | Rigaku corporation, North America  |
| Attachments     | Standard Powder XRD attachment, RxRy attachment, Phi-Chi attachment                                      |
| X ray generator | A 3 kW sealed tube x-ray generator   |
| Optics          | Cross beam optics  |
| Detectors       | 1. 0D Scintillation Counter (point detector), 2. 1D Semiconductor Detector D/tex Ultra (linear detector) |

❖ **Field Emission Scanning Electron Microscope**



|                             |   |
|-----------------------------|---|
| <b>Make</b>                 | Carl Zeiss NTS GmbH, Germany  |
| <b>Model</b>                | <i>SUPRA 55</i>   |
| <b>Resolution</b>           | 1.0 nm @ 15 kV<br>1.7 nm @ 1 kV<br>4.0 nm @ 0.1 kV  |
| <b>Acceleration Voltage</b> | 0.1 – 30 kV   |
| <b>Magnification</b>        | 12x – 900,000 x   |
| <b>Stages</b>               | 5-Axes Motorized Eucentric<br>Specimen Stage X = 130 mm, Y =<br>130 mm and Z = 50 mm, T = -3° to +<br>70°, R = 360° |